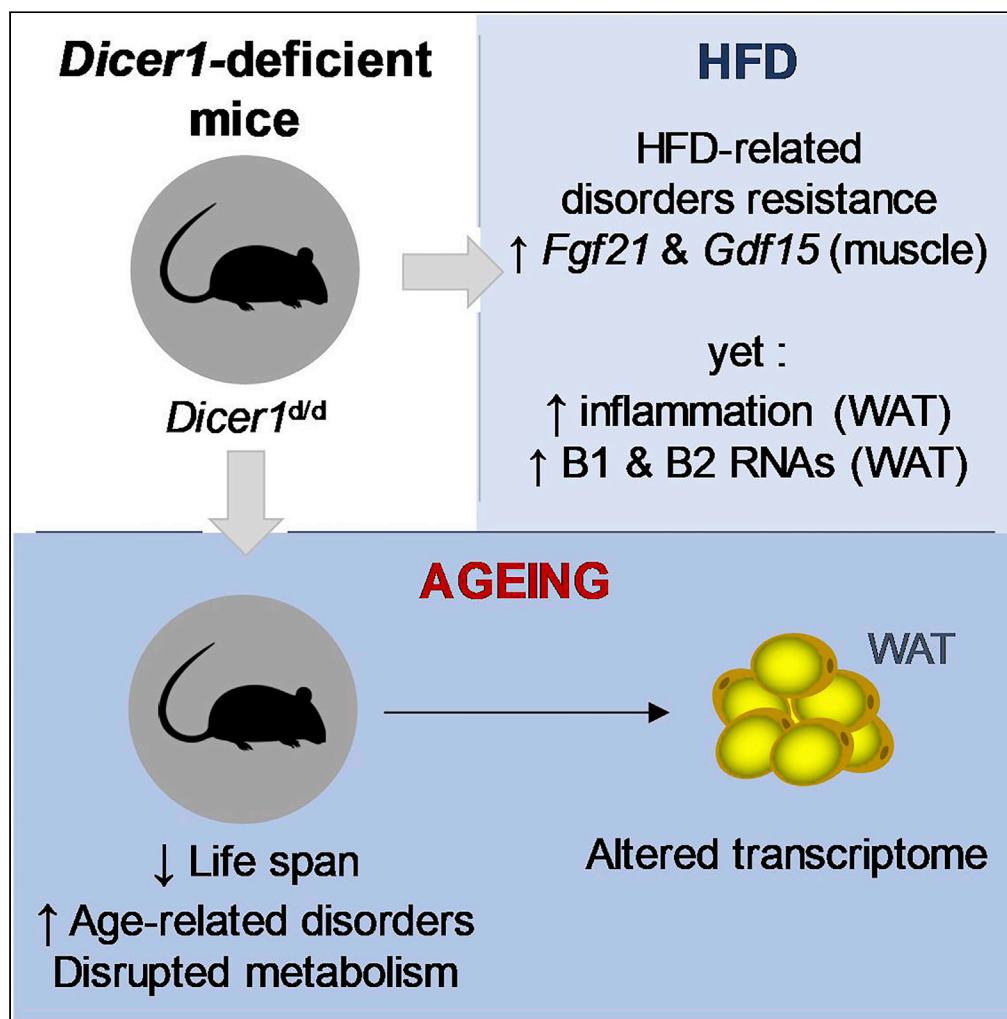


Article

Dicer1 deficient mice exhibit premature aging and metabolic perturbations in adipocytes

Aurore De Cauwer, Thomas Loustau, William Erne, ..., Gertraud Orend, Seiamak Bahram, Philippe Georgel

pgeorgel@unistra.fr

Highlights

Dicer1-deficient mice have a reduced lifespan with early age-related symptoms

Mutant mice are resistant to high fat diet-induced disorders

Myokines FGF21 and GDF15 are likely key regulators of adipocytes metabolism

Article

Dicer1 deficient mice exhibit premature aging and metabolic perturbations in adipocytes

Aurore De Cauwer,¹ Thomas Loustau,¹ William Erne,¹ Angélique Pichot,¹ Anne Molitor,¹ Tristan Stemmelen,^{1,2} Raphael Carapito,^{1,2} Gertraud Orend,¹ Seiamak Bahram,^{1,2} and Philippe Georgel^{1,3,*}

SUMMARY

Age-related diseases are major concern in developed countries. To avoid disabilities that accompany increased lifespan, pharmaceutical approaches are considered. Therefore, appropriate animal models are required for a better understanding of aging processes and potential *in vivo* assays to evaluate the impact of molecules that may delay the occurrence of age-related diseases. Few mouse models exhibiting pathological aging exist, but currently, none of them reproducibly mimics human diseases like osteoporosis, cognitive dysfunctions or sarcopenia that can be seen in some, but not all, elders. Here, we describe the premature aging phenotypes of Dicer-deficient mature animals, which exhibit an overall deterioration of many organs and tissues (skin, heart, and adipose tissue) ultimately leading to a significant reduction of their lifespan. Molecular characterization of transcriptional responses focused on the adipose tissue suggested that both canonical and non-canonical functions of DICER are involved in this process and highlight potential actionable pathways to revert it.

INTRODUCTION

Aging can be defined at the molecular, cellular or organismal levels but its most understandable and tangible definition is the inevitable, time-dependent “physiological deterioration”. Indeed, several changes that accumulate with time are quite obvious: hair loss, cognitive decline, reduced reproductive capacities, impaired muscle strength, to cite a few. Yet, these manifestations are highly variable and while “super-agers” (people in their 70s and 80s who have the mental or physical capability of their decades-younger counterparts) with preserved memory (or physical) performance abilities were described (Sun et al., 2016), others exhibit accelerated deteriorations, as that seen, in the most extreme cases, in progeria patients (Ahmed et al., 2018). This illustrates that our current knowledge of aging is still limited and providing a universal description of this process and its markers remains a challenging task (de Magalhaes and Passos, 2018; Johnson and Stolzing, 2019; Neves and Sousa-Victor, 2019). This points to the necessity to better describe the molecular and cellular processes that are at play during aging *in vivo*.

A crucial observation which sustains aging and the limitation of lifespan is the finite capacity of mammalian cells to divide (Hayflick and Moorhead, 1961), which led to the concept of “cellular senescence” characterized by permanent withdrawal from the cell cycle and acquisition of a pro-inflammatory, proteolytic secretome (Childs et al., 2017). This chronic low-grade inflammatory phenotype, or “inflammaging” (a term defining a biomarker, not interchangeable with “immunosenescence” (Pawelec et al., 2020)), is postulated to be an important contributor to tissue dysfunctions that accompanies age-related decline (van Deursen, 2014). Of note, a causal relationship between inflammation and aging has not yet been formally established. Several stressors, such as reactive oxygen species (ROS) or DNA damage are known inducers of senescence, but it has also recently been suggested that the accumulation of self-molecules (which are normally processed and eliminated by mechanisms such as autophagy) might be an important source of inflammation (Franceschi et al., 2017). In this regard, the role of DICER1 appears of particular importance. DICER1 is essentially known for its canonical role in the RNAi pathway through processing of pre-miRNA transcripts into mature miRNAs (Ha and Kim, 2014). However, additional (non-canonical) functions have been attributed to this RNase III, among which the processing of long non-coding RNAs such as those derived from the transcription of Alu sequences (Song and Rossi, 2017). Although the role of miRNAs in aging has been amply investigated (Kinser and Pincus, 2020), the impact of Alu RNAs accumulation caused

¹Laboratoire d'ImmunoRhumatologie Moléculaire, Institut national de la santé et de la recherche médicale (INSERM) UMR_S 1109, Institut thématique interdisciplinaire (ITI) de Médecine de Précision de Strasbourg, Transplantex NG, Faculté de Médecine, Fédération Hospitalo-Universitaire OMICARE, Fédération de Médecine Translationnelle de Strasbourg (FMTS), Université de Strasbourg, Strasbourg, France

²Laboratoire d'Immunologie, Plateau Technique de Biologie, Pôle de Biologie, Nouvel Hôpital Civil, Strasbourg, France

³Lead contact

*Correspondence: pgeorgel@unistra.fr
<https://doi.org/10.1016/j.isci.2022.105149>



by DICER1 deficiency on inflammation and an age-related disease has been demonstrated in human retinal cells (Gelfand et al., 2015; Kaneko et al., 2011; Kim et al., 2014; Tarallo et al., 2012). Furthermore, recent data in mice (Aryal et al., 2019) (Reis et al., 2016) and in humans (Borras et al., 2017) point to an important contribution of Dicer and other component of the miRNA machinery (Proshkina et al., 2020) in aging. Importantly, mutant mice (*Dicer1^{d/d}*) characterized by reduced *Dicer1* expression are more prone to develop joint inflammation during experimental arthritis (Alsaleh et al., 2016) and have recently been shown to also exhibit age-related macular degeneration (Wright et al., 2020).

In this manuscript, we describe reduced lifespan and increased age-related diseases in *Dicer1^{d/d}* mice. Next, we focused our investigation on the adipose tissue and explored in more details the mechanistic relationships between reduced *Dicer1* expression, inflammation and premature aging. Altogether, our data point to a major role of *Dicer1* in aging, probably through its canonical and non-canonical functions.

RESULTS

Dicer1-deficient mice (*Dicer1^{d/d}*) die prematurely and exhibit age-related diseases

Increased susceptibility to viral infections (Ostermann et al., 2015; Ostermann et al., 2012; Otsuka et al., 2007) and induced colon cancer (Yoshikawa et al., 2013) of *Dicer1^{d/d}* mice have previously been described. However, in the absence of any obvious infectious or tumorigenic trigger (as assessed on careful examination of necropsied animals), we observed a reduced lifespan of *Dicer1^{d/d}* mice (Figure 1A). Animals were kept in the same room of our animal facility and both genotypes (*Dicer1^{+/+}* and *Dicer1^{d/d}*) were co-housed in the same cages to avoid microbiota-specific effects. In these conditions, we could calculate a median survival of 82 weeks for *Dicer1* mutant mice, whereas that of their littermate controls exceeds 2 years. For practical reasons, we could not keep the control animals until their natural death, but the median survival of C57Bl/6J males mice is considered to be of 125 weeks (Kunstyr and Leuenberger, 1975). This means that the average life time of *Dicer1^{d/d}* mice is 35% shorter than controls. Importantly, mutant mice develop more severe and/or more prematurely a morbid state and a set of age-related defects/pathologies. Indeed, aging of mutant mice is accompanied with the development of severe dermatitis (Figure 1B) and kyphosis (Figure 1C), both conditions frequently encountered in aged humans (Ailon et al., 2015; Hahnel et al., 2017) and associated with adverse health effects. Of note, these manifestations were not observed in mice until they were aged at least 40 weeks (Table S1). Additional signs of premature aging were also occasionally seen in *Dicer1^{d/d}* mutants following necropsy (Table S1): conjunctivitis (illustrated Figure 1D) which appears at 90 weeks in normative aging conditions (Coursey et al., 2017), splenomegaly (seen at 80 weeks in aging C57Bl/6 mice (Loukov et al., 2016)), cardiomegaly (starting in 100-week-old C57Bl/6 mice (Eisenberg et al., 2016)) or enlarged seminal vesicles (a feature of 70 week-old mice (Fritz et al., 2005)), although the occurrence of such events was too rare to reach statistical significance. Notably, other defects unrelated to aging, such as alopecia (caused by social behavior (Kalueff et al., 2006)) or rectal prolapses (resulting from intestinal dysbiosis (Buonocore et al., 2010)) were not modified in *Dicer1^{d/d}* mice.

We observed lower body weight of aged mutant mice, a phenotype that can be seen in 60-week-old animals and beyond (Figure 1E). We also noted increased leptin production in the serum of aged wild-type mice, which is in agreement with their elevated body weight (Oswal and Yeo, 2010). Surprisingly however, leptin levels were even higher in 80-week-old *Dicer1* mutants (Figure 1F), despite reduced adipose tissue in these same mice (Figure 1G). Indeed, although control mice gained weight and accumulated fat (which is the main source of leptin) with age, this was not the case in *Dicer1^{d/d}* animals. Importantly, age-dependent weight loss is now considered as a key biological marker of aging and reflects the fragility and vulnerability to pathogens seen in elderly people as well as aged animals (Dutta and Sengupta, 2016). Of note, controls and *Dicer1^{d/d}* mice reach a similar maximum weight (38 g), yet at different times, i.e., week 30 for mutants and week 70 for wild-type animals. The difference (40 weeks) is similar to the loss of life expectancy seen in *Dicer1* mutants. This observation is in line with previous reports showing that the age at which the maximum body weight is reached, rather than the body weight itself, correlates with lifespan (Wagener et al., 2013).

Besides these visible signs, we also quantified several parameters, such as blood pressure and glucose tolerance. As seen in Figure S1, 20 weeks-old *Dicer1^{d/d}* mutants exhibited a slight increase of blood pressure, which appeared significantly augmented in older mice (40- and 80-week-old). This suggests that *Dicer1* deficiency might promote hypertension, a classical feature of aging in humans (Buford, 2016).

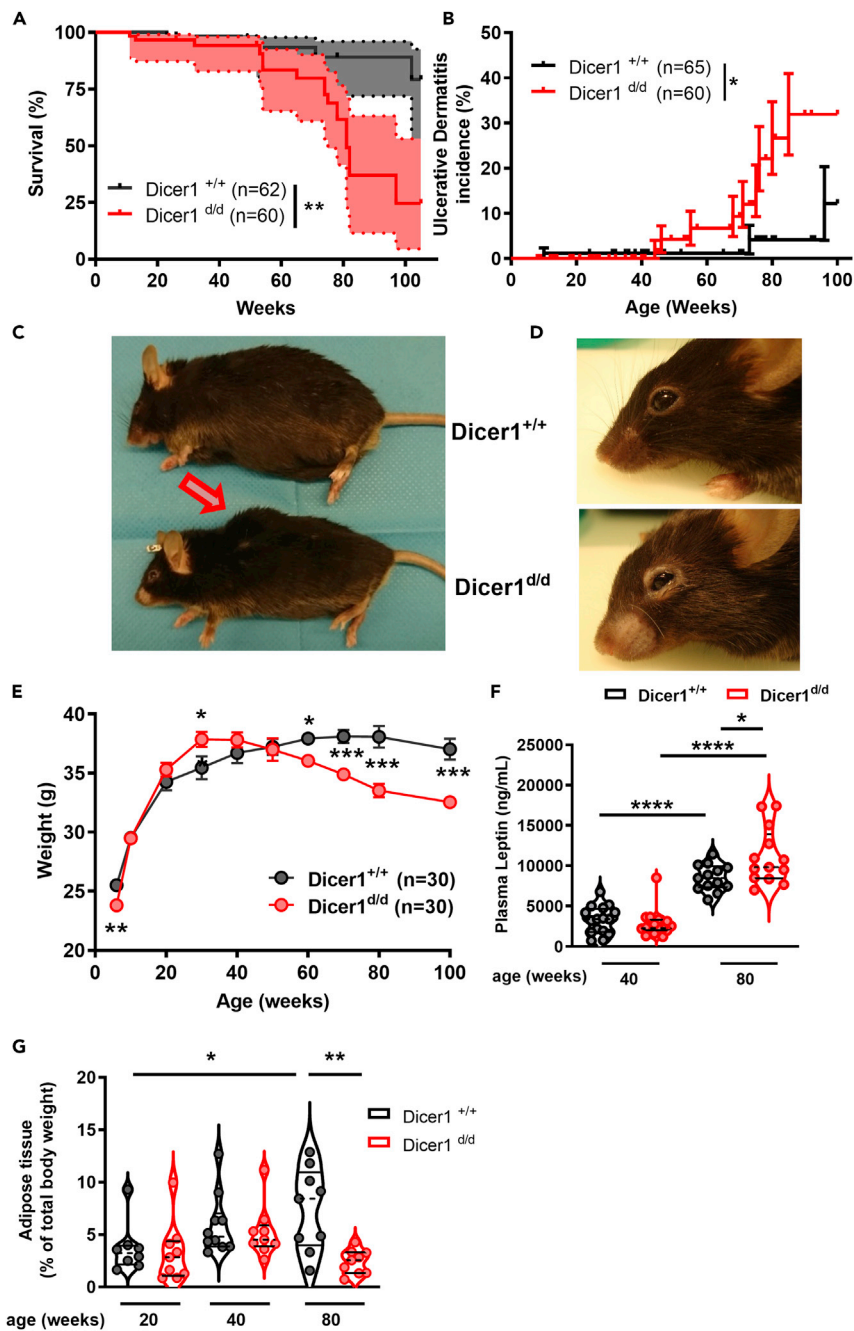


Figure 1. *Dicer1* mutant mice exhibit visible phenotypes evocative of premature aging

(A) The survival of a cohort of 62 wild-type (*Dicer1*^{+/+}) and 60 mutant (*Dicer1*^{d/d}) mice was followed for 80 weeks.
 (B) The occurrence of ulcerative dermatitis was quantified and expressed as a percentage (%) of mutant (60) and control (65) animals showing the phenotype.
 (C) Kyphosis in *Dicer1*^{d/d} mice (bottom) is shown by a red arrow.
 (D) Conjunctivitis in *Dicer1*^{d/d} mice (bottom). Control mice (*Dicer1*^{+/+}) are shown in the top pictures.
 (E) Weight (expressed in grams, g) was measured for 30 controls (*Dicer1*^{+/+}) and 30 mutants (*Dicer1*^{d/d}) for 100 weeks.
 (F) Violin plot showing circulating (Plasma) Leptin (expressed in ng/ml) quantified by ELISA in 40 (N = 16) and 80 weeks-old (N = 13) control and *Dicer1*^{d/d} mice.
 (G) Violin plot showing the amount of adipose tissue (expressed as a percentage of the total body weight) quantified in 20-, 40- and 80-week-old control (*Dicer1*^{+/+}) and mutant (*Dicer1*^{d/d}) mice following necropsy. In panels A and B, data were

Figure 1. Continued

analyzed with the Log-rank test. In panels E, F and G, Data were analyzed by comparing two datasets with a Mann-Whitney U test. * $p < 0.05$; ** $p < 0.01$; *** $p < 0.001$; **** $p < 0.0001$. Data are represented as mean \pm SEM. See also Figure S1 and Table S1.

Altered glucose metabolism in *Dicer1* mutants

To gain more insights into potential metabolic dysfunctions in *Dicer1* mutants, we first performed glucose tolerance tests in cohorts of 20-, 40- and 80-week-old mice. Figure 2 shows that, following intraperitoneal injection (performed in mice that were fasted for 5 h), glucose clearance is more efficient in *Dicer1*-deficient animals, regardless of their age, as determined by the measure of the area under the curve (AUC) (Panels A to C, i and ii). However, we also noted that glycemia is significantly reduced 15 min after glucose injection only in 80-week-old *Dicer1* mutants compared to wild-types (Panel Ci), suggesting increased glucose tolerance in these animals. In addition, fasting glycemia is systematically reduced in *Dicer1*^{d/d} mice (iii). Noticeably, ELISA quantification of plasma insulin showed increased levels in 80-week-old *Dicer1* mutants (Figure 3A), in line with improved glucose clearance. Next, we realized an Insulin Tolerance Test (ITT) and observed a steady glycemia 30 min following insulin injection in fasting 40 weeks-old *Dicer1*-deficient mice (panels B and C), suggesting premature unresponsiveness. Indeed, 80-week-old animals of both genotypes also appeared unresponsive, likely reflecting an age-dependent effect, as seen by others (Ehrhardt et al., 2019). Inconsistencies between our observations and those of others reporting normal glucose metabolism in mice carrying another *Dicer1* hypomorphic mutation (Morita et al., 2009) or hyperglycemia in pancreas-specific *Dicer1* KO mice (Martinez-Sanchez et al., 2015), likely reflect differences in animal models and *Dicer* expression levels. Nevertheless our data illustrate an interesting paradoxical situation whereas insulin resistance should drive hyperglycemia and obesity, our *Dicer1*^{d/d} mice exhibit the opposite phenotype.

Adipose tissue dysfunctions in *Dicer1*^{d/d} mice

Defects in glucose homeostasis seen in aged *Dicer* mutant animals, in conjunction with reduced body weight (Figure 1), pointed to changes in the energetic balance toward consumption, rather than synthesis or storage of nutrients. SIRT1 is a key regulator of energy production through its involvement in insulin secretion as well as maturation and remodeling of the adipose tissue (Hui et al., 2017). Furthermore, *Sirt1* reduced expression in muscle, liver, brain, and adipose tissue has been observed during aging (Gong et al., 2014). Of interest, we observed diminished *Sirt1* expression in the epididymal white adipose tissue (eWAT) of *Dicer1*^{d/d} mice (Figure 4B). Energy metabolism occurs in mitochondria in which glucose and lipid degradation enables ATP production, a process that can be influenced by Un-Coupling Proteins (UCP). In humans, increased *UCP1* expression in visceral adipose tissue is associated with more efficient glucose uptake, reduced blood glycemia and triglyceride levels, combined to a diminished ratio of visceral/subcutaneous adipose tissue (Lim et al., 2020; Tews et al., 2019). Of note, 20 weeks-old *Dicer1* mutant mice exhibit increased *Ucp1* expression in eWAT (Figure 4C). Such changes in *SIRT1* and *UCP1* gene expression in the visceral adipose tissue have been observed in obese patients and might induce metabolic dysfunctions in order to adapt to excessive nutrients availability (Lim et al., 2020). However, a chronic hyper activation of the energy metabolism also induces pathogenic situations, such as cachexia on increased expression of *Ucp1* (Petruzzelli et al., 2014). In addition, activation of the NLRP3 inflammasome drives reduced *Sirt1* expression (Chalkiadaki and Guarente, 2012) and *Ucp1* increased expression is the consequence of ROS production (Han et al., 2016). Of interest, accumulation of SINEs transcripts (B1 and B2 RNAs in mice) resulting from reduced *DICER* expression has been shown to promote NLRP3-dependent inflammation in retinal cells, thereby inducing age-related macular degeneration (Kaneko et al., 2011; Kim et al., 2014; Tarallo et al., 2012). As seen in Figures 4D and 4E, B1 and B2 RNAs accumulate in eWAT, in young as well as in aged *Dicer1* mutants compared to controls. This important observation indicates that this phenomenon, not restricted to the retinal pigment epithelial cells, could potentially represent a more conserved mechanism linking reduced *Dicer1* expression, increased inflammation and aging.

Because *Dicer1* mutants likely exhibit altered metabolic responses in the white adipose tissue, we decided to analyze their behavior in response to high fat diet (HFD) challenge. In these experiments, 10-week-old wild-type and *Dicer1*-deficient mice were subjected to an obesogenic diet for 9 weeks. In these conditions, *Dicer1*-deficient mice exhibited a surprising resistance to weight gain and adipose tissue expansion (Figures 5A–5C). Unexpectedly, *Dicer1*-deficient animals ingested more food than littermate controls and had an increased caloric intake (Figure 5D). In addition, histological examination of the epididymal white adipose tissue shows that adipocytes from *Dicer1*-deficient animals are significantly smaller compared to controls (Figures 5E and 5F).

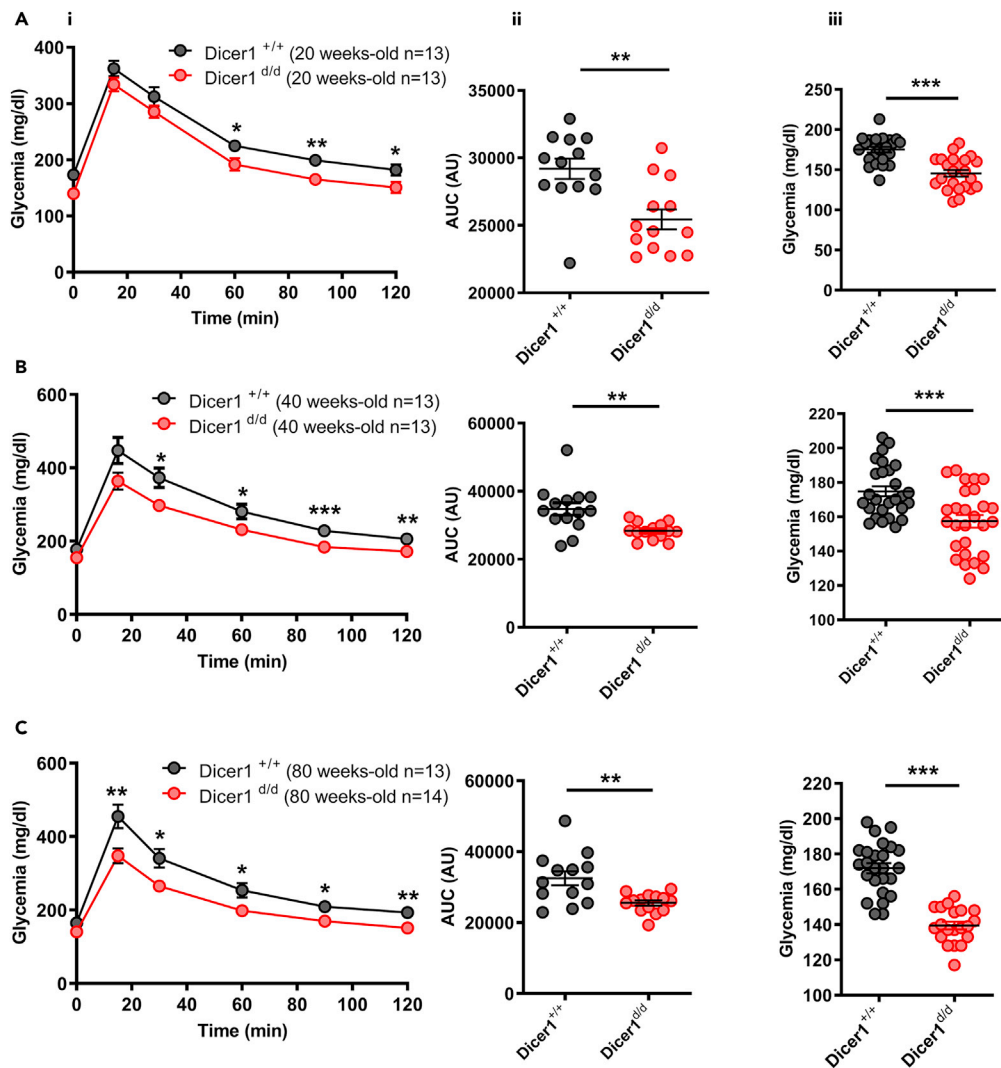


Figure 2. *Dicer1* mutant mice exhibit improved clearance in a glucose tolerance test

(A) Glucose tolerance assay performed in control (*Dicer1*^{+/+}, N = 13) and mutant (*Dicer1*^{d/d}, N = 13) 20-week-old mice. (1) After Glucose intraperitoneal (ip) injection, glycemia (expressed in mg/dL) was quantified during a 120 min (min) period. Wild-type and mutant mice were compared at each time point using an unpaired t-test. (2) The area under the curve (AUC, expressed in arbitrary units-AU) was calculated and differences between wild-types and mutants was analyzed with and unpaired t-test. (3) Quantification of the fasting glycemia (expressed in mg/dL) in the same animals and differences between wild-types and mutants was analyzed with and unpaired t-test. (B) Similar experiments were performed in 40-week-old mice. (C) Similar experiments were performed in 80-week-old mice. *p<0.05; **p<0.01; ***p<0.001. Data are represented as mean ± SEM.

Such chronic exposure to an excess of nutrients induced an increased fasting glycemia and blood insulin concentration in wild-type mice (Figures 6A and 6B), whereas *Dicer1*^{d/d} animals appeared resistant, maintaining a reduced basal glycemia and exhibiting a limited rise in plasma insulin levels. Glucose tolerance tests also showed that *Dicer1*^{d/d} mice exhibited a markedly improved glucose clearance even 8 weeks post HFD (Figures 6C and 6D).

Because HFD is known to induce inflammatory stress in adipocytes, we quantified by RT-qPCR the expression levels of prominent inflammatory markers. As seen in Figure 7A, *Il-1β*, *Il-6*, *Il-18* and *Tnf-α* gene expression is markedly increased in the adipose tissue harvested from *Dicer1*^{d/d} mice subjected to HFD. Importantly, the expression of *B1* and *B2* RNAs also appeared increased in these samples (Figure 7B).

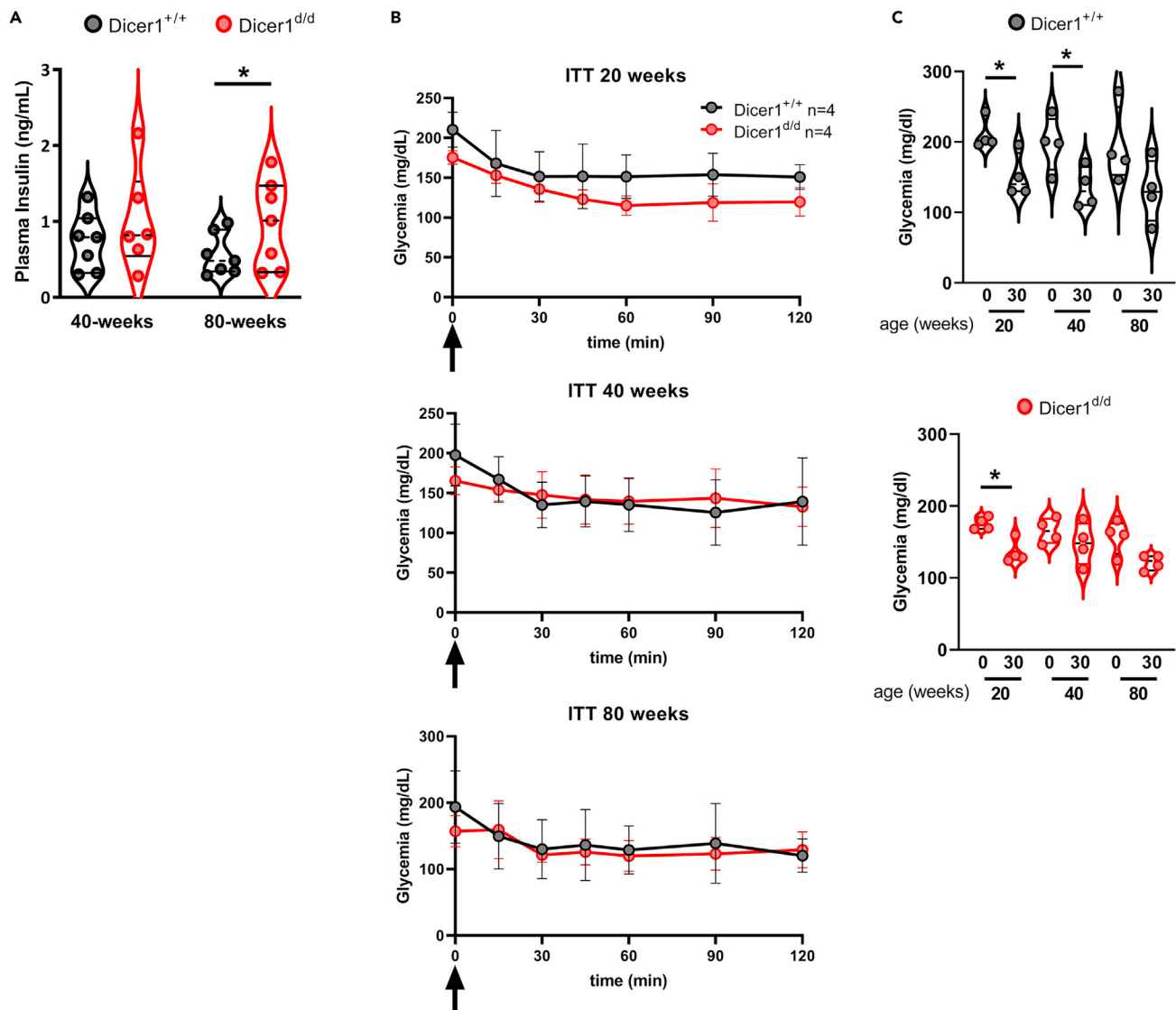


Figure 3. Insulin-resistance in *Dicer1* mutant mice

(A) Violin plot showing the quantification of blood insulin (expressed in ng/ml) by ELISA in 40 and 80 weeks-old wild-type (*Dicer1*^{+/+}, N = 7) and mutants (*Dicer1*^{d/d}, N = 6 or N = 7). Statistical significance is evaluated with a Mann-Whitney U test.

(B) Insulin-tolerance test (ITT). Following insulin ip injection in fasting 20-, 40- and 80-week-old wild-type (*Dicer1*^{+/+}, N = 4) and mutants (*Dicer1*^{d/d}, N = 4), glucose (expressed in mg/dL) was quantified in the blood after 15, 30, 45, 60, 90 and 120 min (min).

(C) Violin plots showing glycemia values at 0 and 30 min after insulin injection in 20-, 40- and 80-week-old *Dicer1*^{+/+} (top) and *Dicer1*^{d/d} (bottom) animals. Data were analyzed with a Mann-Whitney U test. *p<0.05. Data are represented as mean ± SEM.

Yet, targeted gene expression analysis did not provide answers regarding the reduced amount of adipose tissue in *Dicer* mutants. Indeed, expression of β -oxidation genes (*cdvl*, *Acox1*, *Hadha*, *Hadhb*), of mitochondrial respiratory chain (*Idh3a*, *Ogdh*, *Sdh*, *Uqcrcq*), of intestinal barrier integrity (*Zo1*, *Ocl*, *Muc2*) remained comparable in mutants and wt tissues. Furthermore, no liver steatosis could be observed in necropsied animals.

The myokines FGF21 and GDF15 were recently reported as endocrine, stress induced factors capable of establishing a functional crosstalk with the adipose tissue, respectively inducing energy expenditure and reducing food intake and body weight (Keipert and Ost, 2021). Interestingly, we observed increased *Fgf21* and *Gdf15* expression in muscle tissue harvested from 20-week-old *Dicer1* mutant mice compared to controls under normal (chow) diet (Figure 7C). Of note, high fat diet also promoted increased expression

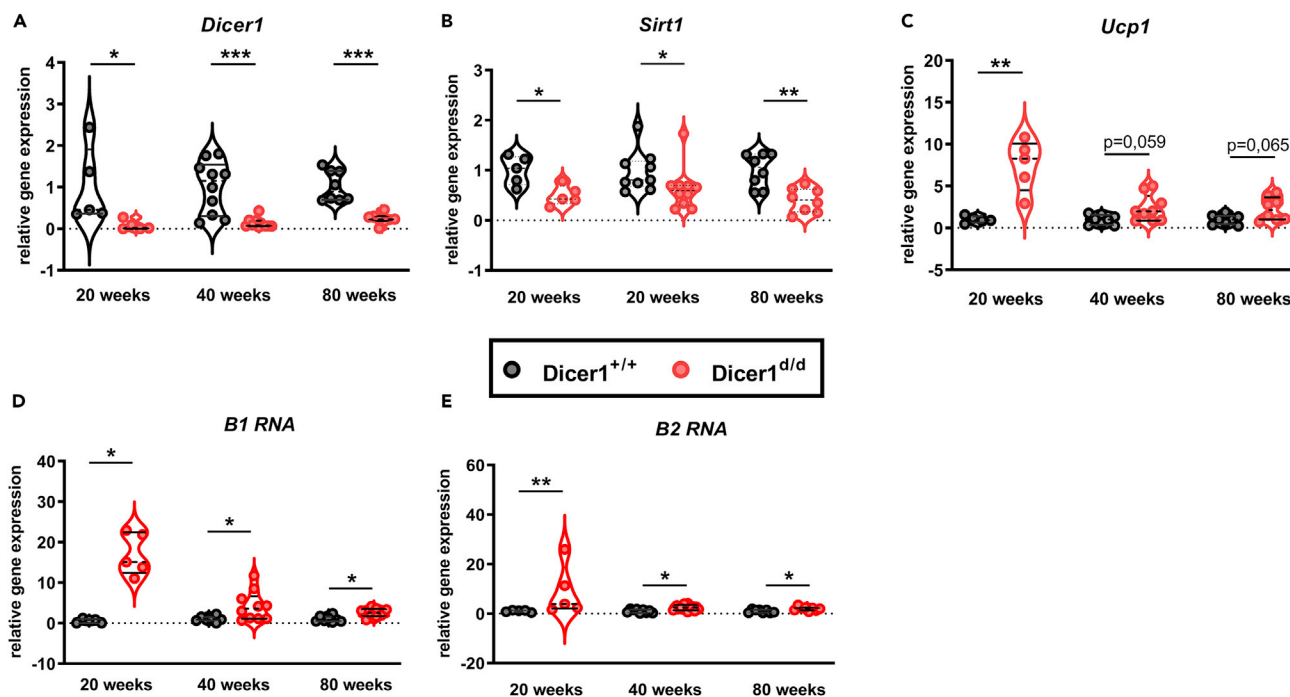


Figure 4. *Dicer1*-specific changes in adipose tissue gene expression

(A–E) *Dicer1*, B. *Sirt1*, C. *Ucp1*, D. *B1 RNA* and E. *B2 RNA* transcripts were quantified by RT-qPCR in the epididymal white adipose tissue of wild-type (*Dicer1*^{+/+}) and mutants (*Dicer1*^{d/d}). Data, represented in violin plots, were analyzed using a Mann-Whitney U test. **p* < 0.05; ***p* < 0.01; ****p* < 0.001. Data are represented as mean ± SEM.

of *Gdf15* in *Dicer1*^{d/d} mice. These data, although preliminary, provide additional insights in favor of the involvement of these factors in the metabolic disturbances seen in *Dicer1*-deficient animals.

Finally, we used an RNAseq approach to obtain a more comprehensive view of the changes in gene expression that occur in adipocytes during aging and evaluate the concomitant impact of reduced *Dicer1* expression. A first hint into global transcriptomic changes is illustrated by the Volcano plots in Figure S2. Panel A shows that aging (in that case between 20 and 80 weeks) of adipocytes in control (wild-type) mice is accompanied by a statistically significant (*P* adj < 0.01) up regulation (2-fold) of 31 genes and down regulation (2-fold) of 52 genes. In contrast, 792 genes are upregulated and 151 down regulated in 80-week-old, compared to 20-week-old *Dicer1*^{d/d} mice (Panel B). Of interest, only 9 genes are differentially expressed between 20-week-old *Dicer1* mutants compared to controls, clearly showing that the mutation has almost no impact in this tissue in young animals (Panel C). This is in sharp contrast to the comparison between 80 weeks-old *Dicer1*^{d/d} and controls (Panel D), which reveals that the expression of 747 genes is increased, whilst that of 99 is reduced. To stratify some of the relevant genes which exhibit differential gene expression, we used heatmap representations and performed Ingenuity Pathways Analysis (IPA, Qiagen) and Gene Set Enrichment Analysis (GSEA, <http://www.webgestalt.org/>). Using these tools, we first managed to highlight several genes involved in aging of wild-type adipocytes (Figure S3), among which HNF4A (Hepatocyte Nuclear Factor 4 Alpha) and Pyruvate Kinase L/R (PKLR) that participate in the Maturity Onset Diabetes of Young (MODY) Signaling and are down-regulated in aged mice. Of note, reduced *Hnf4a* expression has been noted in pancreatic islet of aged rats (Sandovici et al., 2011). Because of the limited amount of differentially expressed genes, GSEA did not allow to identify specific enrichment in gene sets, which likely indicates that 80-week-old animals does probably not really correspond to an advanced age in these wild-type mice. The second dataset that we analyzed compared aged to young *Dicer1*^{d/d} mice (Figure S4). IPA revealed, amongst the top affected pathways, the apelin signaling pathway (*p* = 1.44 × 10⁻⁴). Given the role of the adipokine apelin and its receptor in age-related diseases (Luo et al., 2020; Vinel et al., 2018), reduced expression of both genes in aged *Dicer1*-deficient adipocytes appears particularly relevant and interesting. In addition, GSEA pointed to significant (FDR < 0.05) negative Normalized Enrichment Scores (NES) for gene sets involved in biological processes such as ossification, tissue migration or response to wounding which reflects an ongoing aging process. For

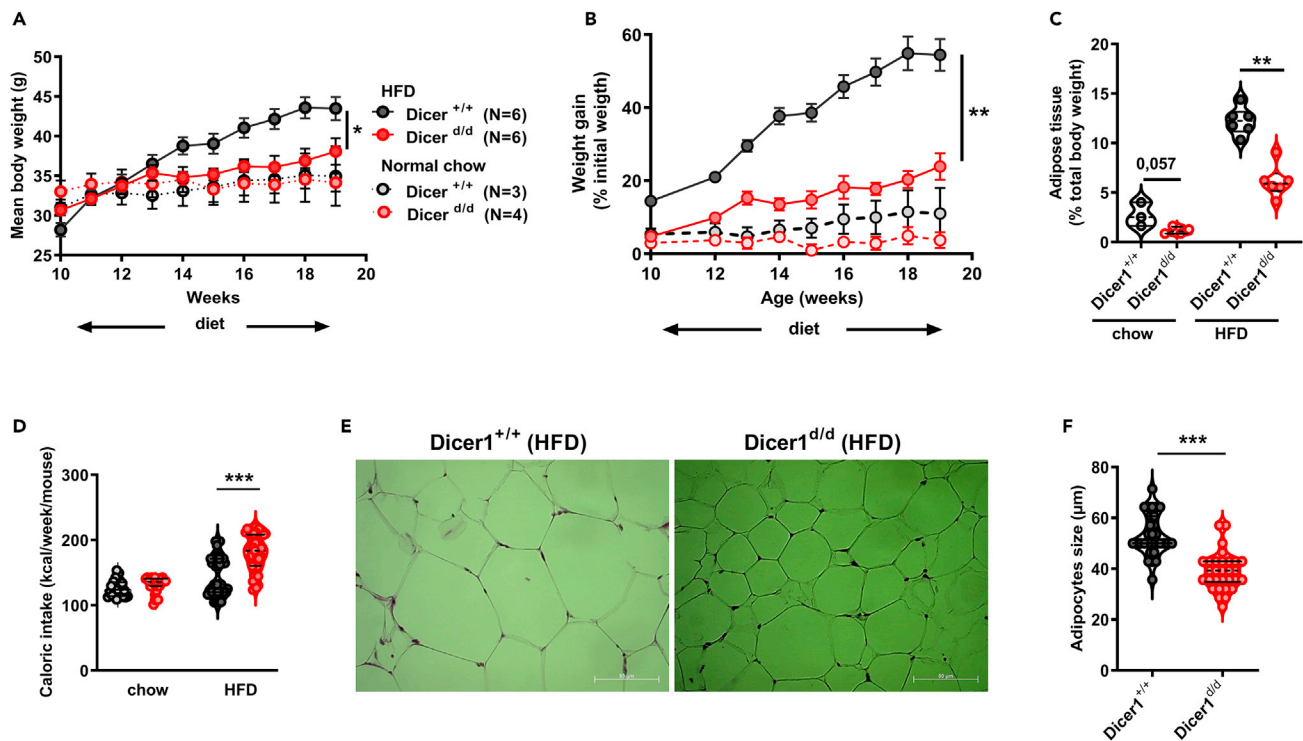


Figure 5. *Dicer1* mutants are resistant to high fat diet

(A and B) Absolute weight (expressed in grams, g) or B. expressed as a percentage of the initial weight was measured in 10-week-old wild-type (*Dicer1*^{+/+}) and mutants (*Dicer1*^{d/d}) mice fed with normal (chow) or high fat (HFD) diet for 9 weeks.

(C) The amount of white adipose tissue (expressed as a percentage of the body mass) was measured in selected wild-type (*Dicer1*^{+/+}) and mutants (*Dicer1*^{d/d}) mice at the end of the experiment.

(D) The caloric intake (expressed in kcal/week/mouse) was measured in the course of the experiment for wild-type (*Dicer1*^{+/+}) and mutants (*Dicer1*^{d/d}) animals.

(E) Histological examination of epididymal white adipose tissue harvested from a wild-type (*Dicer1*^{+/+}) and mutant (*Dicer1*^{d/d}) mouse 9 weeks after high fat diet (HFD) and following hematoxylin/eosin staining.

(F) Quantification of the size (expressed in µm) of the adipocytes from control (*Dicer1*^{+/+}) and mutant (*Dicer1*^{d/d}) adipocytes on HFD. Data, represented as violin plots, were analyzed using a Mann-Whitney U test. Curves in panels A and B were compared following determination of the area under the curve.

p*<0.05; *p*<0.01; ****p*<0.001. Data are represented as mean ± SEM.

instance, the gene set involved in ossification (NES= -2.31; FDR= 0.0019949) includes leptin (*Lep*), Secreted acidic cysteine rich glycoprotein (*Sparc*), Noggin (*Nog*), Collagen, type I, alpha 1 (*Col1a1*), Refilin B (*Rflnb*), Transformation related protein 53 inducible nuclear protein 2 (*Trp53inp2*), Asporin (*Asp*) and cAMP responsive element binding protein 3-like 1 (*Creb3l1*). We also noted the down regulation of several genes encoding extracellular matrix components (Collagens, Tenascin-C), which is also a hallmark of aging (Birch, 2018). Altogether, these data point to premature aging phenotype in these mutant mice, as a result of reduced expression of many genes involved in tissue renewal and homeostasis. A first comparison applied to adipocytes harvested from young animals exhibited only minor changes, mostly involved in interferon signaling, as seen in Figure S5. On the contrary, when we compared the transcriptome of aged mutant adipocytes to that of controls (Figure S6), IPA identified overexpressed genes such as aldolase or glyceraldehyde-3P dehydrogenase that highlighted deregulation of metabolic pathways (panel B) such as gluconeogenesis (*p* = 3.7 × 10⁻⁵) or glycolysis (*p* = 4.2 × 10⁻⁴) in mutant adipocytes. Furthermore, diseases (dermatological, injury) which were identified by IPA (panel C) in this dataset are evocative of ageing-associated processes. GSEA also identified negative NES for genes involved in immune functions (phagocytosis, cytokine production, panel D) or tissue homeostasis, correlating with negative NES indicating abnormal skeleton physiology or immune responses (panel E). Neither in these datasets, nor by RTqPCR could we detect *Dicer1*-specific transcriptional changes in beta-oxidation (*Acdvl*, *Acox1*, *Hadha*, *Hadhb*, not shown) genes expression. Along with the absence of steatotic liver in 80 weeks-old *Dicer1*^{d/d} mice, the metabolic reason for the “lean” phenotype seen in mutants remains unanswered and will require additional investigations.

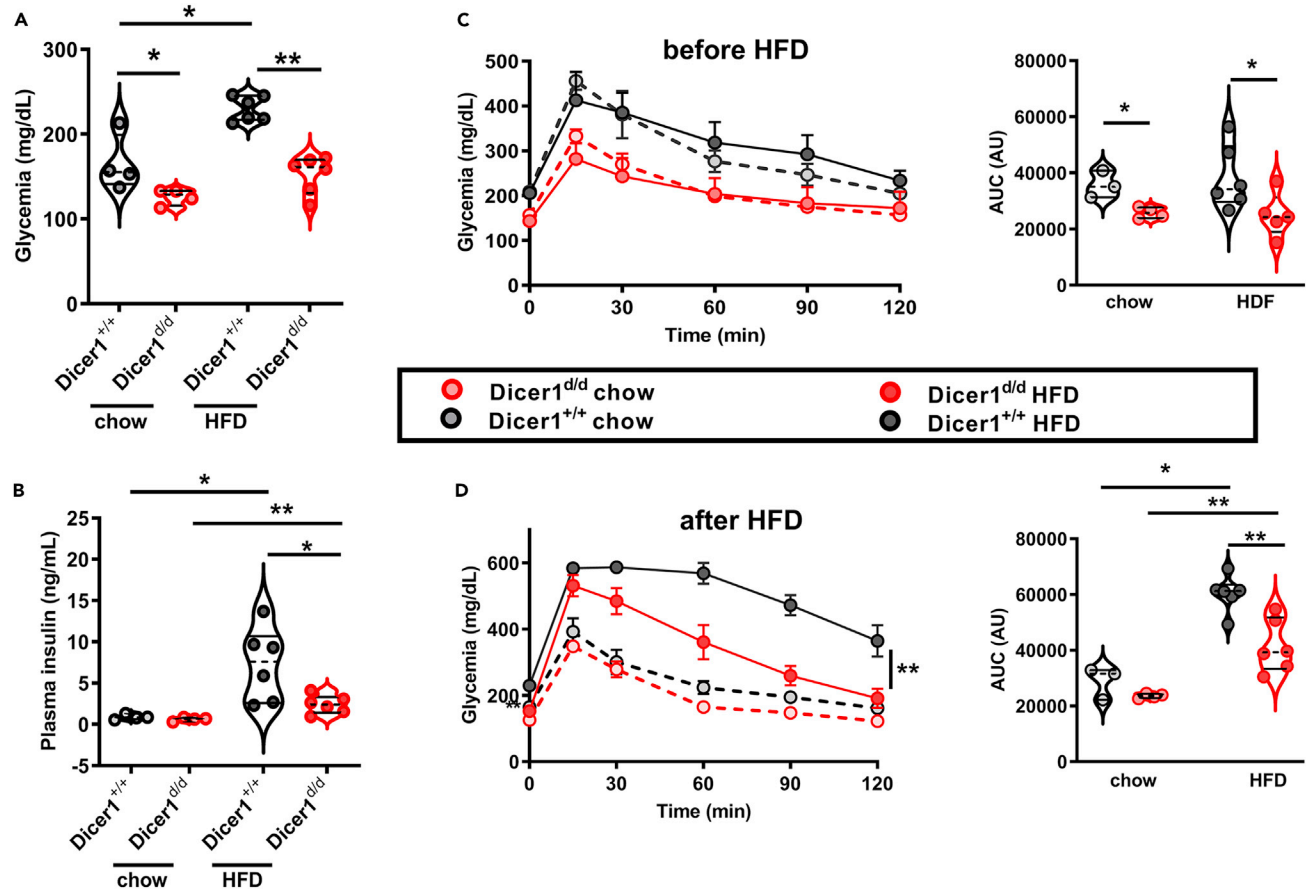


Figure 6. Improved glucose tolerance in *Dicer1* mutants after HFD

(A) Fasting glycemia in the blood (expressed in mg/dL) of wild-type (*Dicer1*^{+/+}) and mutants (*Dicer1*^{d/d}) animals following normal (chow) or high fat diet (HFD).

(B) Blood insulin (expressed in ng/ml) was quantified by ELISA in the same animals as in A.

(C) Glucose tolerance test before high fat diet regimen. Blood glucose (expressed in mg/dL) following glucose ip injection was quantified for 120 min (min) in wild-type (*Dicer1*^{+/+}, in gray) and mutant (*Dicer1*^{d/d}, in red) 10 weeks-old animals that will be fed with normal (chow, dotted line) or high fat diet (HFD, plain line). The right panel shows the area under the curve (AUC, expressed in arbitrary units-AU).

(D) Same experiment as in C was performed in mice following 9 weeks of normal (chow, dotted line) or high fat diet (HFD, plain line). Data, represented as violin plots, were analyzed with a Mann Whitney U test. **p*<0.05; ***p*<0.01. Data are represented as mean ± SEM.

In line with these observations, analysis of our RNAseq data with ImmQuant (Frishberg et al., 2016) revealed that in contrast to wild-type aged mice in which the adipose tissue exhibits increased NKT cells and eosinophils and a reduced number of immune cells progenitors and pDCs, aged *Dicer1*^{d/d} mutants are characterized by more Pro and Early B-cells as well as CD8⁺ effector memory cells infiltrating this tissue (Figure S7), likely contributing to the senescence-associated secretory phenotype (Frasca et al., 2021).

DISCUSSION

Dicer1^{d/d} mice, a relevant model for aging studies

Several animal models have been developed to investigate aging at cellular, molecular and system levels, among which mice exhibit many advantages due to physiological and genetic similarities with humans. However, genetically engineered mice with modified (reduced or increased) lifespan either mimic extreme phenotypes (such as progeroid syndromes which are extremely rare in humans) or affect targeted functions (such as inflammation, metabolism or DNA repair) or specific organs (adipose tissue, liver) (Koks et al., 2016). *Dicer1*-deficient mice appear as an attractive alternative for several reasons: (1) Mutant mice exhibit many defects affecting many organs (retina (Wright et al., 2020); joints (Alsaleh et al., 2016); ovaries (Otsuka et al., 2008); skin and adipose tissue (this study) and, as demonstrated here, are also characterized by

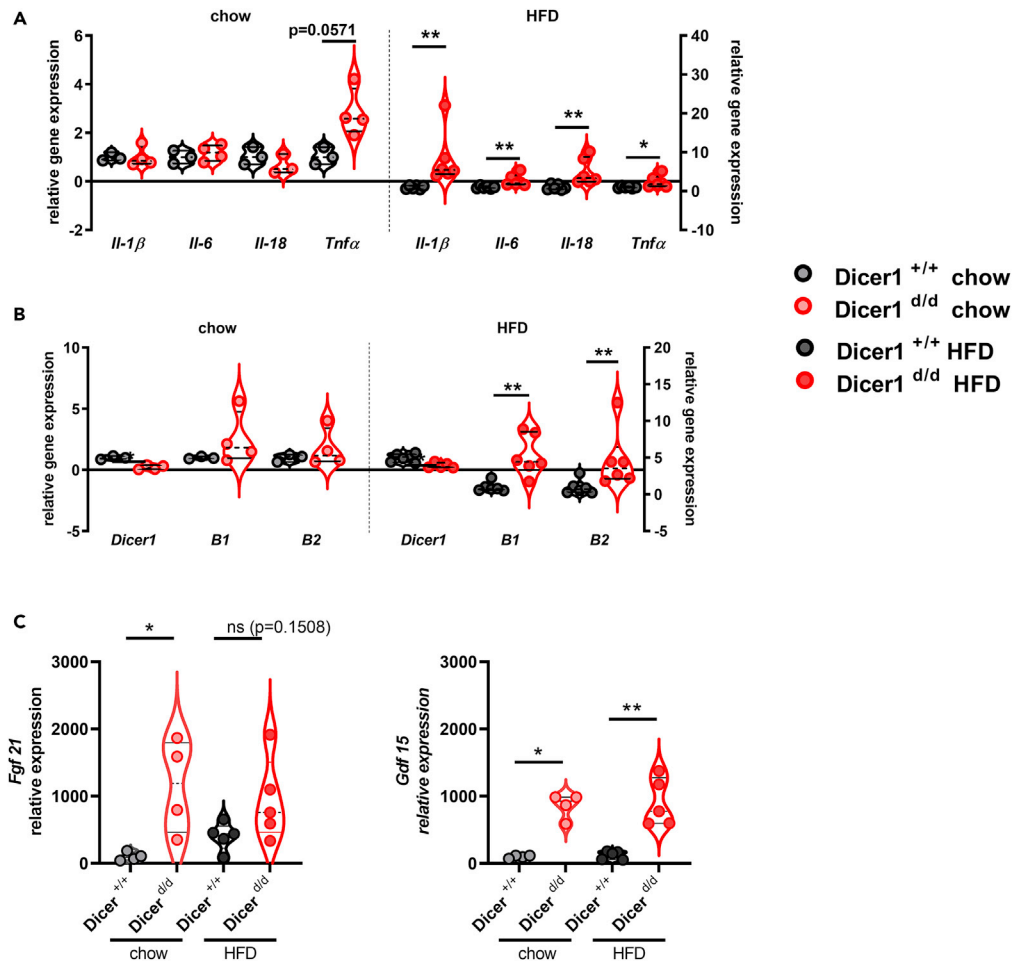


Figure 7. Increased inflammatory signature in *Dicer1* mutant adipocytes on high fat diet

(A) Relative gene expression of inflammatory genes (*Il-1 β* , *Il-6*, *Il-18* and *Tnf α*) quantified by RT-qPCR in the epididymal adipose tissue harvested from wild-type (*Dicer1*^{+/+}) and mutants (*Dicer1*^{d/d}) animals following normal (chow) or high fat diet (HFD).

(B) Relative quantification of *Dicer1*, *B1* and *B2* transcripts in the same conditions as in A.

(C) Relative quantification of *Fgf21* and *Gdf15* gene expression in the quadriceps muscle of 20 weeks-old wild-type (*Dicer1*^{+/+}) and mutants (*Dicer1*^{d/d}) animals, on normal (chow) or high fat diet (HFD). Data, represented in violin plots, were analyzed with a Mann-Whitney U test. * $p < 0.05$; ** $p < 0.01$. Data are represented as mean \pm SEM. See also Figures S2–S7.

reduced lifespan (Figure 1). Of course, more investigations will be necessary to explore in more details phenotypes (like kyphosis) observed in aged *Dicer1*^{d/d} mice. These future studies will enable a better understanding of age-related pathologies (osteoarthritis) of major importance in humans. (2) *Dicer1*^{d/d} mice are hypomorphic, which means that the animals exhibit only a reduced *Dicer1* expression. Indeed, gene deletions are uncommon in humans, in which diversity is more caused by genetic variations and subsequent changes in gene expression and/or activity. In addition, the mutation, which affects pre-mRNA splicing (Otsuka et al., 2007), induces inter-individual heterogeneity, as demonstrated by variable *Dicer* transcript levels between mutant mice, and with one animal, between organs; whereas such variations make the analysis of *Dicer1*^{d/d} mice complex (requiring large cohorts), they mimic the wide spectrum of age-related phenotypes in humans in which aging is not an evolution with stereotypic features. (3) The dynamic of appearance of the phenotypes seen in *Dicer1*^{d/d} mice is evocative of an accelerated aging. Indeed, we could calculate that 50% of *Dicer1*-deficient mice can reach an age (80 weeks) which is equivalent to 62 years for humans (Dutta and Sengupta, 2016), while 50% of the controls can reach 120 weeks (92 years for humans). This likely represents the physiological evolution and diversity seen in human populations. Our findings are in line with observations made using another knock-in mouse model in which DICER1 activity was

reduced by constitutive phosphorylation (Aryal et al., 2019). Of note, accelerated aging, kyphosis and reduced abdominal fat were also observed in this model. Using embryonic fibroblasts, the authors reported increased metabolic rates, possibly explaining fat reduction. Finally, another hypomorphic *Dicer1*-deficient mice has been generated (Morita et al., 2009) and exhibited histological abnormalities in the pancreas, leaving all the other organs intact. These differences likely illustrate the phenotypic variability inherent to hypomorphic mutations, a feature that has been already discussed in the case of *Dicer*^{d/d} mice (Ostermann et al., 2012; Otsuka et al., 2007). On the other hand, to circumvent the embryonic lethality caused by *Dicer* deficiency, conditional, tissue-specific *Dicer* KO mice have been generated using the CRE/lox technology. Initial observations were made in isolated murine pre-adipocytes in which *Dicer* ablation was obtained on transduction of a CRE-expressing adenovirus (Mori et al., 2012). In these cells, increased sensitivity to cells stressors and gene expression analysis suggested that *Dicer* ablation promoted senescence. Conditional *Dicer* KO mice were also generated and exhibited reduced survival rate following oxidative stress induction by paraquat injection. Of interest, identical conditional *Dicer* KO mice (using the aP2-Cre driver) were analyzed by two different groups (Mori et al., 2014; Mudhasani et al., 2011), who observed severe post-natal lethality, a feature that was attributed to off-target effects and Cre expression in non-adipose tissues. In contrast, using the adiponectin promoter to drive Cre expression (Mori et al., 2014), mutant mice exhibited lipodystrophy, loss of white fat and insulin resistance, phenotypes that are also seen in our *Dicer*^{d/d} mice. Finally, we would like to stress that our observations in mice are in line with human data showing that centenarians, exhibiting delayed aging, are characterized by miRNA and *Dicer* overexpression compared to octogenarians with ordinary aging features (Borras et al., 2017). Altogether, these data point to an important role of *Dicer* in the adipose tissue and for a healthy organism.

Nevertheless, the mechanism by which *Dicer1*-reduced expression triggers premature aging remains to be fully elucidated. A first clue is the overexpression of *B1* and *B2* RNAs detected in adipocytes of *Dicer1*^{d/d} mice fed with a lipid-rich diet (Figure 4). This observation, in line with those performed in retinal epithelial pigment cells (Kaneko et al., 2011; Kim et al., 2014; Tarallo et al., 2012), suggests that non-canonical functions of DICER1 (Alu sequences processing) could participate in the inflammatory setting of adipocytes and mediate the inflammaging phenotype. Alternatively, reduced *Dicer1* expression also entails an impairment of nuclear DICER1 functions, such as the maintenance of telomeres or the response to DNA damages (Burger and Gullerova, 2015), whose dysfunction might also drive cellular senescence. Finally, the canonical role of DICER1 (i.e, the maturation of miRNAs) is certainly an important player in the accelerated aging seen in *Dicer1*^{d/d} mice. This is visualized by the large number of deregulated genes in adipocytes harvested from aged mutant mice compared to controls. Indeed, many of these genes might be under transcriptional control by miRNAs, as demonstrated by others (Mori et al., 2014).

Transcriptomic analyses of adipocytes highlight multiple pathways involved in aging

Adipocytes have long been under-estimated and explored for their energy storage functions only. Yet, the adipose tissue represents an important proportion (20%, depending on age, sex) of the total body mass in humans (Jackson et al., 2012) (30% in mice, depending on strains (Reed et al., 2007)) and is able to secrete many signaling molecules (adipokines) involved in the regulation of multiple processes like wounding (Lee et al., 2018), bone density (Reid et al., 2018) or immune responses (Francisco et al., 2018). Furthermore, the relationships between lipid metabolism and age-related disease appear more and more functionally related (Arai et al., 2019). To better characterize the changes that occur in these cells during aging and the impact of reduced *Dicer1* expression in this process at the molecular level, we performed a transcriptomic analyses by RNAseq. First, we focused on "normal" aging by comparing gene expression levels between 80 weeks-old and 20 weeks-old wild-type mice (Figure S3). Setting the cutoff for significant changes to a $p \text{ adj} < 0.01$ and a minimal fold change of 2, we found few (83) deregulated genes, which likely indicates that 80 weeks does not correspond to old animals, but rather to "mature adults" which are not so different, at least with regards to the adipose tissue, from 20-week-old, "young adults". Nevertheless, we observed that the top pathways which were predicted to be deregulated by IPA play a role in glucose metabolism. Importantly, the MODY pathway is among them, in line with premature diabetes and insulin-resistance, two importance features of aging. We also observed increased expression of several immunoglobulin-encoding genes, possibly reflecting the accumulation of B cells in the adipose tissue during aging, as previously reported (Camell et al., 2019). Of interest, GSEA highlighted the reduced expression of many genes encoding components of the extracellular matrix (Tenascin-C, various Collagens, Asporin) in *Dicer1*^{d/d} mice. Such alterations drive probably the most visible effect of aging in humans, the loss of skin elasticity and the

appearance of wrinkles. Surprisingly, the comparison of 20 weeks-old *Dicer1* mutants and age-matched controls (Figure S4) revealed almost no difference (8 differentially expressed genes), except an overexpression of *Irf7* and *Ifit1* genes, evocative of an interferon signature that we described earlier (Ostermann et al., 2012). Transcriptomic differences were much more marked when we compared 80 and 20 weeks-old *Dicer1^{d/d}* adipocytes (Figure S5) and highlighted several deregulated genes (*Nrep*, *Fabp3*, *Col1a1*, *H1f2*, *Lyz1*, *Col3a1*, *B2m*, *S100a4*) common to human, rat and mouse which are listed in the Human Aging Genomic Resources database (<https://genomics.senescence.info/>) (de Magalhaes et al., 2009). Several deregulated metabolic pathways were identified by IPA (i.e., neoglucogenesis), as well as the Apelin signaling cascade (shown panel B). Indeed, reduced expression of Apelin and its receptor have been recently described as important events promoting senescence (Zhou et al., 2018). GSEA identified significant (FDR<0.05) negative enrichment scores for genes participating in processes such as ossification or response to wounding (panel C), providing additional evidence of accelerated aging in *Dicer1* mutants. Finally, we analyzed the impact of *Dicer1*-reduced expression in aged animals and compared 80-week-old mutants to age-matched controls (Figure S6). First, we noted that most genes were up-regulated (Figure S2D), reflecting the reduced expression of miRs (which exhibit essentially negative regulatory roles) as a result of low DICER1 levels. Next, IPA confirmed the deregulation of metabolic pathways (gluconeogenesis, glycolysis) that occurs in *Dicer1*-deficient aged animals and GSEA confirmed the negative enrichment of genes participating in extracellular matrix and phenotypes (immune, bone-related), reflecting an overall degradation of major physiological functions and premature aging. Interestingly, we also showed that *Dicer* deficiency, by reducing *Fgf21* and *Gdf15* expression in muscles (Figure 7C), impacts endocrine signaling emanating from this tissue, thereby participating in altered lipid metabolism and feeding behavior seen in mutant animals. Of course, more work will be necessary to uncover the changes in muscle/adipocytes connections that results from *Dicer1*-reduced expression.

Delaying aging and the occurrence of age-related diseases

The proportion of elderly is constantly increasing in developed countries. This aging population is at risk to develop chronic diseases, such as cardiovascular, rheumatic and neurodegenerative conditions, thereby creating a massive economic burden to the social security systems. Hence, the development of drugs enabling enhanced lifespan, in the absence of age-related diseases is a major challenge and the focus of intense research. To this end, rejuvenation strategies are considered and can be divided into two main categories: (1) Those that are based on dietary restriction and (2) the ablation of senescent cells by chemotherapy (senolytics) (Mahmoudi et al., 2019). In this work, we showed that high fat diet (HFD) promoted enhanced inflammatory genes expression in *Dicer1* mutant mice (Figure 7). Concomitantly, we observed that *Dicer1^{d/d}* mice are also resistant to adipogenesis and weight gain in these conditions (Figure 5) and are still able to control their glycemia better than wild-type animals (Figure 6). These contrasting observations will require additional investigations, like a quantification of lipid absorption in the intestinal lumen. However, they can be connected to recent observations in humans suggesting that a reduced BMI is associated with a greater risk of mortality in elderly (Winter et al., 2014). In this work, neither did we evaluate the impact of HFD on mortality in *Dicer1* mutants, nor the consequences of diet restrictions. These experiments will have to be performed in the future.

An important message from our transcriptomic analyses is the potential impact of adipokines on the accelerated aging seen in *Dicer1^{d/d}* mice. Indeed, in addition to apelin and its receptor, the genes encoding leptin, resistin, chemerin are also down regulated in aged mutant animals. These observations suggest that, in addition to senolytics (Xu et al., 2018) or anti-inflammatory molecules (Neves and Sousa-Victor, 2020), the modulation of physiological processes such as food intake or energy expenditure by adipokines (which also possess some neuroprotective activities (Arnoldussen et al., 2014) might become an attractive pharmacological tool to enhance lifespan in healthy conditions.

In conclusion, our work enabled us to provide a comprehensive description of the functions of *Dicer1* in adipocytes and during aging. Although still imperfectly characterized, *Dicer1^{d/d}* mice might represent a physiologically-relevant model to thoroughly investigate aging *in vivo* and evaluate the efficacy of molecules which will be used in humans to postpone the occurrence of age-related diseases.

Limitations of the study

This study is essentially observational and premature aging seen in *Dicer1*-deficient mutants needs to be sustained by biochemical, histological (e.g., SA- β -Gal staining) and molecular (telomere length)

investigations to consider senescence as a mechanism accounting for the observed phenotypes. Furthermore, metabolic perturbations suggested by our transcriptomic analysis of adipocytes should be documented with measures of energy expenditure to better apprehend the subsequent mechanisms driven by reduced *Dicer1* expression. Finally, quantification of microRNAs expression, with our transcriptomic analysis, should enable the identification of miRNA-regulated mRNAs in adipocytes.

STAR★METHODS

Detailed methods are provided in the online version of this paper and include the following:

- KEY RESOURCES TABLE
- RESOURCE AVAILABILITY
 - Lead contact
 - Materials availability
 - Data and code availability
- EXPERIMENTAL MODEL AND SUBJECT DETAILS
 - *Dicer1*-deficient mouse line
 - Housing and husbandry
- METHOD DETAILS
 - High fat diet (HFD)
 - Glucose/insulin tolerance test
 - Insulin and leptin quantification
 - Adipose tissue quantification
 - Histological analysis
 - RT-qPCR
 - RNA-sequencing
 - Analysis of RNA-seq data
- QUANTIFICATION AND STATISTICAL ANALYSIS

SUPPLEMENTAL INFORMATION

Supplemental information can be found online at <https://doi.org/10.1016/j.isci.2022.105149>.

ACKNOWLEDGMENTS

Technical help from Fanny Steinbach for histology and Cécile Macquin for mouse work is acknowledged. We also thank Nicodème Paul for help and advice in statistical analysis. Work in SB laboratory is supported by the Strasbourg's Interdisciplinary Thematic Institute (ITI) for Precision Medicine, TRANSPLANTEX NG, as part of the ITI 2021-2028 program of the University of Strasbourg, CNRS and Inserm, funded by IdEx Unistra (ANR-10-IDEX-0002) and SFRI-STRAT'US (ANR-20-SFRI-0012), the INSERM UMR_S 1109, the University of Strasbourg (IDEX UNISTRA), the European regional development fund (European Union) INTERREG V program (project PERSONALIS) and the MSD-Avenir grant AUTOGEN. GO is supported by ANR-PRCI MatrixNash, Aviesan ITMO cancer project Radio 3R and INCa PLBIO project TENMAX. ADC and WE were recipients of a fellowship from the French Ministry of Research and Technology.

AUTHOR CONTRIBUTIONS

Conceptualization, A.D.C. and P.G.; Investigation, A.D.C., T.L., W.E., and A.P.; Formal analysis, A.D.C., A.M., T.S., R.C., and P.G.; Resources, R.C., G.O., and S.B.; Writing – Original draft, A.D.C. and P.G.; Writing – Review and editing: A.D.C., R.C., G.O., S.B., and P.G.; Funding acquisition, G.O. and S.B.; Supervision, P.G.. All authors have reviewed and agreed to this information before submission.

DECLARATION OF INTERESTS

The authors declare no competing interest.

Received: February 3, 2022

Revised: August 12, 2022

Accepted: September 13, 2022

Published: October 21, 2022

REFERENCES

- Ahmed, M.S., Ikram, S., Bibi, N., and Mir, A. (2018). Hutchinson-gilford progeria syndrome: a premature aging disease. *Mol. Neurobiol.* 55, 4417–4427. <https://doi.org/10.1007/s12035-017-0610-7>.
- Ailon, T., Shaffrey, C.I., Lenke, L.G., Harrop, J.S., and Smith, J.S. (2015). Progressive spinal kyphosis in the aging population. *Neurosurgery 77 (Suppl 4)*, S164–S172. <https://doi.org/10.1227/NEU.0000000000000944>.
- Alsaleh, G., Nehmar, R., Blüml, S., Schleiss, C., Ostermann, E., Dillenseger, J.P., Sayeh, A., Choquet, P., Dembele, D., Francois, A., et al. (2016). Reduced DICER1 expression bestows rheumatoid arthritis synovocytes proinflammatory properties and resistance to apoptotic stimuli. *Arthritis Rheumatol.* 68, 1839–1848. <https://doi.org/10.1002/art.39641>.
- Anders, S., Pyl, P.T., and Huber, W. (2015). HTSeq—a Python framework to work with high-throughput sequencing data. *Bioinformatics* 31, 166–169. <https://doi.org/10.1093/bioinformatics/btu638>.
- Arai, Y., Kamide, K., and Hirose, N. (2019). Adipokines and aging: findings from centenarians and the very old. *Front. Endocrinol.* 10, 142. <https://doi.org/10.3389/fendo.2019.00142>.
- Arnoldussen, I.A.C., Kiliaan, A.J., and Gustafson, D.R. (2014). Obesity and dementia: adipokines interact with the brain. *Eur. Neuropsychopharmacol.* 24, 1982–1999. <https://doi.org/10.1016/j.euroneuro.2014.03.002>.
- Aryal, N.K., Pant, V., Wasylishen, A.R., Parker-Thornburg, J., Baseler, L., El-Naggar, A.K., Liu, B., Kalia, A., Lozano, G., and Arur, S. (2019). Constitutive Dicer1 phosphorylation accelerates metabolism and aging in vivo. *Proc. Natl. Acad. Sci. USA* 116, 960–969. <https://doi.org/10.1073/pnas.1814377116>.
- Birch, H.L. (2018). Extracellular matrix and ageing. *Subcell. Biochem.* 90, 169–190. https://doi.org/10.1007/978-981-13-2835-0_7.
- Borrás, C., Serna, E., Gambini, J., Inglés, M., and Vina, J. (2017). Centenarians maintain miRNA biogenesis pathway while it is impaired in octogenarians. *Mech. Ageing Dev.* 168, 54–57. <https://doi.org/10.1016/j.mad.2017.07.003>.
- Burford, T.W. (2016). Hypertension and aging. *Ageing Res. Rev.* 26, 96–111. <https://doi.org/10.1016/j.arr.2016.01.007>.
- Buonocore, S., Ahern, P.P., Uhlig, H.H., Powrie, F., Ivanov, I.I., Ivanov, I.I., Littman, D.R., and Maloy, K.J. (2010). Innate lymphoid cells drive interleukin-23-dependent innate intestinal pathology. *Nature* 464, 1371–1375. <https://doi.org/10.1038/nature08949>.
- Burger, K., and Gullerova, M. (2015). Swiss army knives: non-canonical functions of nuclear Drosha and Dicer. *Nat. Rev. Mol. Cell Biol.* 16, 417–430. <https://doi.org/10.1038/nrm3994>.
- Camell, C.D., Günther, P., Lee, A., Goldberg, E.L., Spadaro, O., Youm, Y.H., Bartke, A., Hubbard, G.B., Ikeno, Y., Ruddle, N.H., et al. (2019). Aging induces an Nlrp3 inflammasome-dependent expansion of adipose B cells that impairs metabolic homeostasis. *Cell Metab.* 30, 1024–1039.e6. <https://doi.org/10.1016/j.cmet.2019.10.006>.
- Chalkiadaki, A., and Guarente, L. (2012). High-fat diet triggers inflammation-induced cleavage of SIRT1 in adipose tissue to promote metabolic dysfunction. *Cell Metab.* 16, 180–188. <https://doi.org/10.1016/j.cmet.2012.07.003>.
- Childs, B.G., Gluscevic, M., Baker, D.J., Laberge, R.M., Marquess, D., Dananberg, J., and van Deursen, J.M. (2017). Senescent cells: an emerging target for diseases of ageing. *Nat. Rev. Drug Discov.* 16, 718–735. <https://doi.org/10.1038/nrd.2017.116>.
- Coursey, T.G., Bian, F., Zaheer, M., Pflugfelder, S.C., Volpe, E.A., and de Paiva, C.S. (2017). Age-related spontaneous lacrimal keratoconjunctivitis is accompanied by dysfunctional T regulatory cells. *Mucosal Immunol.* 10, 743–756. <https://doi.org/10.1038/mi.2016.83>.
- de Magalhães, J.P., Curado, J., and Church, G.M. (2009). Meta-analysis of age-related gene expression profiles identifies common signatures of aging. *Bioinformatics* 25, 875–881. <https://doi.org/10.1093/bioinformatics/btp073>.
- de Magalhães, J.P., and Passos, J.F. (2018). Stress, cell senescence and organismal ageing. *Mech. Ageing Dev.* 170, 2–9. <https://doi.org/10.1016/j.mad.2017.07.001>.
- Dobin, A., Davis, C.A., Schlesinger, F., Drenkow, J., Zaleski, C., Jha, S., Batut, P., Chaisson, M., and Gingeras, T.R. (2013). STAR: ultrafast universal RNA-seq aligner. *Bioinformatics* 29, 15–21. <https://doi.org/10.1093/bioinformatics/bts635>.
- Dutta, S., and Sengupta, P. (2016). Men and mice: relating their ages. *Life Sci.* 152, 244–248. <https://doi.org/10.1016/j.lfs.2015.10.025>.
- Ehrhardt, N., Cui, J., Dagdeviren, S., Saengnipanthkul, S., Goodridge, H.S., Kim, J.K., Lantier, L., Guo, X., Chen, Y.D.I., Raffel, L.J., et al. (2019). Adiposity-independent effects of aging on insulin sensitivity and clearance in mice and humans. *Obesity* 27, 434–443. <https://doi.org/10.1002/oby.22418>.
- Eisenberg, T., Abdellatif, M., Schroeder, S., Primessnig, U., Stekovic, S., Pendl, T., Harger, A., Schipke, J., Zimmermann, A., Schmidt, A., et al. (2016). Cardioprotection and lifespan extension by the natural polyamine spermidine. *Nat. Med.* 22, 1428–1438. <https://doi.org/10.1038/nm.4222>.
- Franceschi, C., Garagnani, P., Vitale, G., Capri, M., and Salvioli, S. (2017). Inflammaging and ‘Garb-aging’. *Trends Endocrinol. Metab.* 28, 199–212. <https://doi.org/10.1016/j.tem.2016.09.005>.
- Francisco, V., Pino, J., Gonzalez-Gay, M.A., Mera, A., Lago, F., Gómez, R., Mobasher, A., and Gualillo, O. (2018). Adipokines and inflammation: is it a question of weight? *Br. J. Pharmacol.* 175, 1569–1579. <https://doi.org/10.1111/bph.14181>.
- Frasca, D., Romero, M., Diaz, A., Garcia, D., Thaller, S., and Blomberg, B.B. (2021). B cells with a senescent-associated secretory phenotype Accumulate in the adipose tissue of individuals with obesity. *Int. J. Mol. Sci.* 22, 1839. <https://doi.org/10.3390/ijms22041839>.
- Frishberg, A., Brodt, A., Steuerma, Y., and Gat-Viks, I. (2016). ImmQuant: a user-friendly tool for inferring immune cell-type composition from gene-expression data. *Bioinformatics* 32, 3842–3843. <https://doi.org/10.1093/bioinformatics/btw535>.
- Fritz, W.A., Lin, T.M., Moore, R.W., Cooke, P.S., and Peterson, R.E. (2005). In utero and lactational 2, 3, 7, 8-tetrachlorodibenzo-p-dioxin exposure: effects on the prostate and its response to castration in senescent C57BL/6J mice. *Toxicol. Sci.* 86, 387–395. <https://doi.org/10.1093/toxsci/kfi189>.
- Gelfand, B.D., Wright, C.B., Kim, Y., Yasuma, T., Yasuma, R., Li, S., Fowler, B.J., Bastos-Carvalho, A., Kerur, N., Uittenbogaard, A., et al. (2015). Iron toxicity in the retina requires Alu RNA and the NLRP3 inflammasome. *Cell Rep.* 11, 1686–1693. <https://doi.org/10.1016/j.celrep.2015.05.023>.
- Gong, H., Pang, J., Han, Y., Dai, Y., Dai, D., Cai, J., and Zhang, T.M. (2014). Age-dependent tissue expression patterns of Sirt1 in senescence-accelerated mice. *Mol. Med. Rep.* 10, 3296–3302. <https://doi.org/10.3892/mmr.2014.2648>.
- Ha, M., and Kim, V.N. (2014). Regulation of microRNA biogenesis. *Nat. Rev. Mol. Cell Biol.* 15, 509–524. <https://doi.org/10.1038/nrm3838>.
- Hahnel, E., Lichterfeld, A., Blume-Peytavi, U., and Kottner, J. (2017). The epidemiology of skin conditions in the aged: a systematic review. *J. Tissue Viability* 26, 20–28. <https://doi.org/10.1016/j.jtv.2016.04.001>.
- Han, Y.H., Buffolo, M., Pires, K.M., Pei, S., Scherer, P.E., and Boudina, S. (2016). Adipocyte-specific deletion of manganese superoxide dismutase protects from diet-induced obesity through increased mitochondrial uncoupling and biogenesis. *Diabetes* 65, 2639–2651. <https://doi.org/10.2337/db16-0283>.
- Hayflick, L., and Moorhead, P.S. (1961). The serial cultivation of human diploid cell strains. *Exp. Cell Res.* 25, 585–621. [https://doi.org/10.1016/0014-4827\(61\)90192-6](https://doi.org/10.1016/0014-4827(61)90192-6).
- Hui, X., Zhang, M., Gu, P., Li, K., Gao, Y., Wu, D., Wang, Y., and Xu, A. (2017). Adipocyte SIRT1 controls systemic insulin sensitivity by modulating macrophages in adipose tissue. *EMBO Rep.* 18, 645–657. <https://doi.org/10.15252/embr.201643184>.
- Jackson, A.S., Janssen, I., Sui, X., Church, T.S., and Blair, S.N. (2012). Longitudinal changes in body composition associated with healthy ageing: men, aged 20–96 years. *Br. J. Nutr.* 107, 1085–1091. <https://doi.org/10.1017/S0007114511003886>.
- Johnson, A.A., and Stolzing, A. (2019). The role of lipid metabolism in aging, lifespan regulation, and age-related disease. *Aging Cell* 18, e13048. <https://doi.org/10.1111/acel.13048>.
- Kalueff, A.V., Minasyan, A., Keisala, T., Shah, Z.H., and Tuohimaa, P. (2006). Hair barbering in

- mice: implications for neurobehavioural research. *Behav. Processes* 71, 8–15. <https://doi.org/10.1016/j.beproc.2005.09.004>.
- Kaneko, H., Dridi, S., Tarallo, V., Gelfand, B.D., Fowler, B.J., Cho, W.G., Kleinman, M.E., Ponicsan, S.L., Hauswirth, W.W., Chiodo, V.A., et al. (2011). DICER1 deficit induces Alu RNA toxicity in age-related macular degeneration. *Nature* 471, 325–330. <https://doi.org/10.1038/nature09830>.
- Keipert, S., and Ost, M. (2021). Stress-induced FGF21 and GDF15 in obesity and obesity resistance. *Trends Endocrinol. Metab.* 32, 904–915. <https://doi.org/10.1016/j.tem.2021.08.008>.
- Kim, Y., Tarallo, V., Kerur, N., Yasuma, T., Gelfand, B.D., Bastos-Carvalho, A., Hirano, Y., Yasuma, R., Mizutani, T., Fowler, B.J., et al. (2014). DICER1/Alu RNA dysmetabolism induces Caspase-8-mediated cell death in age-related macular degeneration. *Proc. Natl. Acad. Sci. USA* 111, 16082–16087. <https://doi.org/10.1073/pnas.1403814111>.
- Kinser, H.E., and Pincus, Z. (2020). MicroRNAs as modulators of longevity and the aging process. *Hum. Genet.* 139, 291–308. <https://doi.org/10.1007/s00439-019-02046-0>.
- Köks, S., Dogan, S., Tuna, B.G., González-Navarro, H., Potter, P., and Vandenbroucke, R.E. (2016). Mouse models of ageing and their relevance to disease. *Mech. Ageing Dev.* 160, 41–53. <https://doi.org/10.1016/j.mad.2016.10.001>.
- Kunstyr, I., and Leuenberger, H.G. (1975). Gerontological data of C57BL/6J mice. I. Sex differences in survival curves. *J. Gerontol.* 30, 157–162. <https://doi.org/10.1093/geronj/30.2.157>.
- Langmead, B., and Salzberg, S.L. (2012). Fast gapped-read alignment with Bowtie 2. *Nat. Methods* 9, 357–359. <https://doi.org/10.1038/nmeth.1923>.
- Lee, B.C., Song, J., Lee, A., Cho, D., and Kim, T.S. (2018). Visfatin promotes wound healing through the activation of ERK1/2 and JNK1/2 pathway. *Int. J. Mol. Sci.* 19, E3642. <https://doi.org/10.3390/ijms19113642>.
- Lim, J., Park, H.S., Kim, J., Jang, Y.J., Kim, J.H., Lee, Y., and Heo, Y. (2020). Depot-specific UCP1 expression in human white adipose tissue and its association with obesity-related markers. *Int. J. Obes.* 44, 697–706. <https://doi.org/10.1038/s41366-020-0528-4>.
- Loukov, D., Naidoo, A., Puchta, A., Marin, J.L.A., and Bowdish, D.M.E. (2016). Tumor necrosis factor drives increased splenic monopoiesis in old mice. *J. Leukoc. Biol.* 100, 121–129. <https://doi.org/10.1189/jlb.3MA0915-433RR>.
- Love, M.I., Huber, W., and Anders, S. (2014). Moderated estimation of fold change and dispersion for RNA-seq data with DESeq2. *Genome Biol.* 15, 550. <https://doi.org/10.1186/s13059-014-0550-8>.
- Luo, H., Han, L., and Xu, J. (2020). Apelin/APJ system: a novel promising target for neurodegenerative diseases. *J. Cell. Physiol.* 235, 638–657. <https://doi.org/10.1002/jcp.29001>.
- Mahmoudi, S., Xu, L., and Brunet, A. (2019). Turning back time with emerging rejuvenation strategies. *Nat. Cell Biol.* 21, 32–43. <https://doi.org/10.1038/s41556-018-0206-0>.
- Martinez-Sanchez, A., Nguyen-Tu, M.S., and Rutter, G.A. (2015). DICER1 inactivation identifies pancreatic beta-cell "Disallowed" genes targeted by MicroRNAs. *Mol. Endocrinol.* 29, 1067–1079. <https://doi.org/10.1210/me.2015-1059>.
- Mori, M.A., Raghavan, P., Thomou, T., Boucher, J., Robida-Stubbs, S., Macotela, Y., Russell, S.J., Kirkland, J.L., Blackwell, T.K., and Kahn, C.R. (2012). Role of microRNA processing in adipose tissue in stress defense and longevity. *Cell Metab.* 16, 336–347. <https://doi.org/10.1016/j.cmet.2012.07.017>.
- Mori, M.A., Thomou, T., Boucher, J., Lee, K.Y., Lallukka, S., Kim, J.K., Torriani, M., Yki-Järvinen, H., Grinspoon, S.K., Cypess, A.M., and Kahn, C.R. (2014). Altered miRNA processing disrupts brown/white adipocyte determination and associates with lipodystrophy. *J. Clin. Invest.* 124, 3339–3351. <https://doi.org/10.1172/JCI73468>.
- Morita, S., Hara, A., Kojima, I., Horii, T., Kimura, M., Kitamura, T., Ochiya, T., Nakanishi, K., Matoba, R., Matsubara, K., and Hatada, I. (2009). Dicer is required for maintaining adult pancreas. *PLoS One* 4, e4212. <https://doi.org/10.1371/journal.pone.0004212>.
- Mudhasani, R., Puri, V., Hoover, K., Czech, M.P., Imbalzano, A.N., and Jones, S.N. (2011). Dicer is required for the formation of white but not brown adipose tissue. *J. Cell. Physiol.* 226, 1399–1406. <https://doi.org/10.1002/jcp.22475>.
- Nehmar, R., Alsaleh, G., Voisin, B., Flacher, V., Mariotte, A., Saferding, V., Puchner, A., Niederreiter, B., Vandamme, T., Schabbauer, G., et al. (2017). Therapeutic modulation of plasmacytoid dendritic cells in experimental arthritis. *Arthritis Rheumatol.* 69, 2124–2135. <https://doi.org/10.1002/art.40225>.
- Neves, J., and Sousa-Victor, P. (2019). Regulation of inflammation as an anti-aging intervention. *FEBS J.* 287, 43–52. <https://doi.org/10.1111/febs.15061>.
- Neves, J., and Sousa-Victor, P. (2020). Regulation of inflammation as an anti-aging intervention. *FEBS J.* 287, 43–52. <https://doi.org/10.1111/febs.15061>.
- Ostermann, E., Macquin, C., Krezel, W., Bahram, S., and Georgel, P. (2015). Increased viral dissemination in the brain and lethality in MCMV-infected, dicer-deficient neonates. *Viruses* 7, 2308–2320. <https://doi.org/10.3390/v7052308>.
- Ostermann, E., Tuddenham, L., Macquin, C., Alsaleh, G., Schreiber-Becker, J., Tanguy, M., Bahram, S., Pfeffer, S., and Georgel, P. (2012). Deregulation of type I IFN-dependent genes correlates with increased susceptibility to cytomegalovirus acute infection of dicer mutant mice. *PLoS One* 7, e43744. <https://doi.org/10.1371/journal.pone.0043744>.
- Oswal, A., and Yeo, G. (2010). Leptin and the control of body weight: a review of its diverse central targets, signaling mechanisms, and role in the pathogenesis of obesity. *Obesity* 18, 221–229. <https://doi.org/10.1038/oby.2009.228>.
- Otsuka, M., Jing, Q., Georgel, P., New, L., Chen, J., Mols, J., Kang, Y.J., Jiang, Z., Du, X., Cook, R., et al. (2007). Hypersusceptibility to vesicular stomatitis virus infection in Dicer1-deficient mice is due to impaired miR24 and miR93 expression. *Immunity* 27, 123–134. <https://doi.org/10.1016/j.immuni.2007.05.014>.
- Otsuka, M., Zheng, M., Hayashi, M., Lee, J.D., Yoshino, O., Lin, S., and Han, J. (2008). Impaired microRNA processing causes corpus luteum insufficiency and infertility in mice. *J. Clin. Invest.* 118, 1944–1954. <https://doi.org/10.1172/JCI33680>.
- Pawelec, G., Bronikowski, A., Cunnane, S.C., Ferrucci, L., Franceschi, C., Fülöp, T., Gaudreau, P., Gladyshev, V.N., Gonos, E.S., Gorbunova, V., et al. (2020). The conundrum of human immune system "senescence". *Mech. Ageing Dev.* 192, 111357. <https://doi.org/10.1016/j.mad.2020.111357>.
- Petrucelli, M., Schweiger, M., Schreiber, R., Campos-Olivas, R., Tsoli, M., Allen, J., Swarbrick, M., Rose-John, S., Rincon, M., Robertson, G., et al. (2014). A switch from white to brown fat increases energy expenditure in cancer-associated cachexia. *Cell Metab.* 20, 433–447. <https://doi.org/10.1016/j.cmet.2014.06.011>.
- Proshkina, E., Solovev, I., Koval, L., and Moskalev, A. (2020). The critical impacts of small RNA biogenesis proteins on aging, longevity and age-related diseases. *Ageing Res. Rev.* 62, 101087. <https://doi.org/10.1016/j.arr.2020.101087>.
- Reed, D.R., Bachmanov, A.A., and Tordoff, M.G. (2007). Forty mouse strain survey of body composition. *Physiol. Behav.* 91, 593–600. <https://doi.org/10.1016/j.physbeh.2007.03.026>.
- Reid, I.R., Baldock, P.A., and Cornish, J. (2018). Effects of leptin on the skeleton. *Endocr. Rev.* 39, 938–959. <https://doi.org/10.1210/er.2017-00226>.
- Reis, F.C.G., Branquinho, J.L.O., Brandão, B.B., Guerra, B.A., Silva, I.D., Frontini, A., Thomou, T., Sartini, L., Cinti, S., Kahn, C.R., et al. (2016). Fat-specific Dicer deficiency accelerates aging and mitigates several effects of dietary restriction in mice. *Aging (Albany NY)* 8, 1201–1222. <https://doi.org/10.18632/aging.100970>.
- Sandovici, I., Smith, N.H., Nitert, M.D., Ackers-Johnson, M., Uribe-Lewis, S., Ito, Y., Jones, R.H., Marquez, V.E., Cairns, W., Tadayyon, M., et al. (2011). Maternal diet and aging alter the epigenetic control of a promoter-enhancer interaction at the Hnf4a gene in rat pancreatic islets. *Proc. Natl. Acad. Sci. USA* 108, 5449–5454. <https://doi.org/10.1073/pnas.1019007108>.
- Song, M.S., and Rossi, J.J. (2017). Molecular mechanisms of Dicer: endonuclease and enzymatic activity. *Biochem. J.* 474, 1603–1618. <https://doi.org/10.1042/BCJ20160759>.
- Sun, F.W., Stepanovic, M.R., Andreano, J., Barrett, L.F., Touroutoglou, A., and Dickerson, B.C. (2016). Youthful brains in older adults: preserved neuroanatomy in the default mode and salience networks contributes to youthful memory in superaging. *J. Neurosci.* 36, 9659–9668. <https://doi.org/10.1523/JNEUROSCI.1492-16.2016>.

Tarallo, V., Hirano, Y., Gelfand, B.D., Dridi, S., Kerur, N., Kim, Y., Cho, W.G., Kaneko, H., Fowler, B.J., Bogdanovich, S., et al. (2012). DICER1 loss and Alu RNA induce age-related macular degeneration via the NLRP3 inflammasome and MyD88. *Cell* 149, 847–859. <https://doi.org/10.1016/j.cell.2012.03.036>.

Tews, D., Pula, T., Funcke, J.B., Jastroch, M., Keuper, M., Debatin, K.M., Wabitsch, M., and Fischer-Posovszky, P. (2019). Elevated UCP1 levels are sufficient to improve glucose uptake in human white adipocytes. *Redox Biol.* 26, 101286. <https://doi.org/10.1016/j.redox.2019.101286>.

van Deursen, J.M. (2014). The role of senescent cells in ageing. *Nature* 509, 439–446. <https://doi.org/10.1038/nature13193>.

Vinel, C., Lukjanenko, L., Batut, A., Deleruyelle, S., Pradère, J.P., Le Gonidec, S., Dortignac, A., Geoffre, N., Pereira, O., Karaz, S., et al. (2018). The

exerkine apelin reverses age-associated sarcopenia. *Nat. Med.* 24, 1360–1371. <https://doi.org/10.1038/s41591-018-0131-6>.

Wagener, A., Müller, U., and Brockmann, G.A. (2013). The age of attaining highest body weight correlates with lifespan in a genetically obese mouse model. *Nutr.Diabetes* 3, e62. <https://doi.org/10.1038/nutd.2013.4>.

Winter, J.E., MacInnis, R.J., Wattanapenpaiboon, N., and Nowson, C.A. (2014). BMI and all-cause mortality in older adults: a meta-analysis. *Am. J. Clin. Nutr.* 99, 875–890. <https://doi.org/10.3945/ajcn.113.068122>.

Wright, C.B., Uehara, H., Kim, Y., Yasuma, T., Yasuma, R., Hirahara, S., Makin, R.D., Apicella, I., Pereira, F., Nagasaka, Y., et al. (2020). Chronic Dicer1 deficiency promotes atrophic and neovascular outer retinal pathologies in mice. *Proc. Natl. Acad. Sci. USA* 117, 2579–

2587. <https://doi.org/10.1073/pnas.1909761117>.

Xu, M., Pirtskhalava, T., Farr, J.N., Weigand, B.M., Palmer, A.K., Weivoda, M.M., Inman, C.L., Ogradnik, M.B., Hachfeld, C.M., Fraser, D.G., et al. (2018). Senolytics improve physical function and increase lifespan in old age. *Nat. Med.* 24, 1246–1256. <https://doi.org/10.1038/s41591-018-0092-9>.

Yoshikawa, T., Otsuka, M., Kishikawa, T., Takata, A., Ohno, M., Shibata, C., Kang, Y.J., Yoshida, H., and Koike, K. (2013). Unique haploinsufficient role of the microRNA-processing molecule Dicer1 in a murine colitis-associated tumorigenesis model. *PLoS One* 8, e71969. <https://doi.org/10.1371/journal.pone.0071969>.

Zhou, Q., Chen, L., Tang, M., Guo, Y., and Li, L. (2018). Apelin/APJ system: a novel promising target for anti-aging intervention. *Clin.Chim. Acta* 487, 233–240. <https://doi.org/10.1016/j.cca.2018.10.011>.

STAR★METHODS

KEY RESOURCES TABLE

REAGENT or RESOURCE	SOURCE	IDENTIFIER
Critical commercial assays		
Custom diet for Rat & Mice, 61% of the energy from fat (lard)	SAFE custom Diets	SAFE® U8954 version 205
Insulin solution human	Sigma-Aldrich	CAS 11061-68-0
Mouse/Rat Leptin Quantikine ELISA Kit	R&D systems	CAT#MOB00
Rat/Mouse Insulin ELISA	Merck	EZRMI-13K
Hematoxylin and Eosin Staining Kit	Abcam	Ab245880
TRlzol® Reagent	Invitrogen	CAT#15596026
IScript™ cDNA Qynthesis Kit	BIO-RAD	1708891
SsoAdvanced Universal SYBR® Green Supermix	BIO-RAD	1725274
Agilent RNA 6000 Pico kit	Agilent	5067-1513
SMARTer Stranded total RNA-seq ki v2 – Pico input mammalian	Takara	634417
Experimental models: Organisms/strains		
<i>Dicer1^{gt(β-geo)han}</i> mouse strain	Otsuka et al., 2007	N/A
Software and algorithms		
FastQC	Babraham Institute	RRID:SCR-014583 http://www.bioinformatics.babraham.ac.uk/projects/fastqc/
Image J		RRID:SCR_003070 https://imagej.net/
STAR	Dobin et al., 2013	RRID:SCR_004463 http://code.google.com/p/rna-star/
Bowtie2	Langmead and Salzberg, 2012	RRID:SCR_016368 http://bowtie-bio.sourceforge.net/bowtie2/index.shtml
HTseq	Anders et al., 2015	RRID:SCR_005514 http://htseq.readthedocs.io/en/release_0.9.1/
DESeq2	Love et al., 2014	RRID:SCR_015687 https://bioconductor.org/packages/release/bioc/html/DESeq2.html
Ingenuity Pathway Analysis IPA	Ingenuity	RRID:SCR_008653
ImmQuant	Frishberg et al., 2016	http://csgi.tau.ac.il/ImmQuant/
Other		
Databases to study the genetics of ageing	Human Ageing Genomic Resources	https://genomics.senescence.info/

RESOURCE AVAILABILITY

Lead contact

Further information and requests for resources and reagents should be directed to and will be fulfilled by the lead contact, Philippe Georgel (pgeorgel@unistra.fr).

Materials availability

This study did not generate new unique reagents.

Data and code availability

- All data reported in this paper will be shared by the [lead contact](#) upon request.
- This paper does not report original code.
- Any additional information required to reanalyze the data reported in this paper is available from the [lead contact](#) upon request.

EXPERIMENTAL MODEL AND SUBJECT DETAILS

Dicer1-deficient mouse line

Dicer1-deficient strain was established by other (Otsuka et al., 2007). Briefly, the model was generated by using a gene-trap method with a β -galactosidase-neomycin (β -geo) insertion in intron 24 of the *Dicer1* locus, abolishing Dicer1's activity. However, a low-frequency alternative splicing event results in a wild-type-processed transcript in *Dicer1*^{d/d} mice, leading to a hypomorphic phenotype (low DICER1 protein expression). The *Dicer1*-deficient strain, backcrossed to C56Bl/6Jcrl (Charles River Laboratories) was maintained in a heterozygous state, and homozygous wild-type and mutant littermates were utilized for the experiments.

Housing and husbandry

All animals were kept under specific pathogen-free conditions in the animal facility of the Center de Recherche d'Hématologie et d'Immunologie. Only males were used in the experiments described in this paper. Unless stated otherwise, mice were housed in groups (2–7 animals) containing both genotypes to minimize potential microbiota-specific effect and were kept under stabilized temperature (20–22°C) with a 12h dark-light cycle and fed water/food *ad libitum*. Cages were enriched with cotton tubes for nests and red polycarbonate tunnels. Handling and experiments were done by a single experimenter, aware of mice genotype at all time. Our experiments were approved by the local ethic committee (CREMEAS, protocol reference APAFIS#21782-2019061317371610 v4).

METHOD DETAILS

High fat diet (HFD)

Ten-week-old males were housed in individually cages and provided with standard food pellets (SAFE, A03) or a high-fat diet (SAFE, 292HF, U8954 60% calories from lipids) and tap water *ad libitum* throughout the study (10 weeks). Animals and food were weight weekly to follow body weight and food consumption. Blood collection on the submandibular vein was performed on conscious animals at week 1 and before sacrifice for Insulin quantification (as described below). An intraperitoneal glucose tolerance test (as described below) was performed at week 1 and week 9.

Glucose/insulin tolerance test

The glucose tolerance of animals was assessed by an intraperitoneal glucose tolerance test (ipGTT) at designated times. Mice were transferred into new clean cage and fasted for 5 h, typically from 8 a.m. to 1 p.m. The first blood samples were collected from tail tip and blood glucose was measured using a glucometer (CareSens), which was considered as time 0 min. Subsequently, a 20% glucose solution was administered intraperitoneally into mice (2 g/kg of body weight) and blood glucose was monitored at 15, 30, 60, 90 and 120 min after glucose administration.

The insulin tolerance was assessed by an intraperitoneal insulin tolerance test (ipITT). After 5 h of fasting, blood samples were collected from the mouse tail tip and blood glucose was measured. Subsequently, mice were intraperitoneally injected with 0.75 U/kg body weight of recombinant human insulin (Sigma-Aldrich). Blood glucose was monitored at 15, 30, 45, 60, 90 and 120 min after insulin administration.

Insulin and leptin quantification

At designed time/age, blood was collected on submandibular vein on conscious animals. Samples were centrifuged at 5000× g for 10 min to separate plasma and stored at –80°C for analysis. Leptin and Insulin concentration were estimated by ELISA following the manufactures' guidelines (Mouse/Rat Leptin Quantikine ELISA Kit, R&D Systems; Rat/Mouse Insulin ELISA kit, Merck Millipore).

Adipose tissue quantification

At described time or age, mice were euthanized by cervical dislocation. Fat depots were immediately collected and weighted to compare visceral (perirenal, epididymal, retroperitoneal) and subcutaneous (dorsolumbar, inguinal) depots. Epididymal white adipose tissue was then processed for freezing in dry ice (protein and mRNA analysis) or for embedding in paraffin (Leica, 39,601,006) after 4% formalin fixation.

Histological analysis

Embedded tissue was then sliced to 8- μ m thickness sections on glass slides, and subjected to Hematoxylin and Eosin staining following manufacturer's instructions (H&E staining kit, Abcam ab245880). Sections were examined using a Zeiss Axio Imager A1; pictures were taken with an Axiocam IC3 and further analyzed using ImageJ software.

RT-qPCR

Total RNA was prepared as described (Nehmar et al., 2017). Briefly, adipose tissue was minced and then grinded into TRIzol reagent for RNA extraction following manufacturer's instructions (Invitrogen N015596026). Total RNA was then reverse transcribed using the cDNA synthesis kit (Biorad). Real-time quantitative RT-qPCR was performed in a total volume of 10 μ L using the Sso-advanced universal SYBR-Green supermix (Biorad) and gene-specific primers (list available upon request). After a denaturing step at 95°C for 30 s, 40 cycles were performed (95°C for 5s and 60°C for 20s) using a Rotor-Gene 6000 real-time PCR machine (Corbett Life Science). Results were obtained using the SDS Software (Perkin Elmer). Melting-curve analysis was performed to assess the specificity of PCR products. Relative expression was calculated using the comparative threshold cycle (Ct) method. The Ct of the gene of interest was adjusted to the average Ct of three housekeeping genes (18S, Actin and Gapdh) to obtain a Δ Ct.

RNA-sequencing

Total RNA integrity was determined with the Agilent total RNA Pico Kit on a 2100 Bioanalyzer instrument (Agilent Technologies, Paolo Alto, USA). Library construction was performed with the SMARTer Stranded Total RNA-Seq Kit v2 - Pico Input Mammalian" (TaKaRa Bio USA, Inc., Mountain View, CA, USA) with a final multiplexing of 11 libraries according to the manufacturer's instructions. The library pool was sequenced on a NextSeq 500 (Illumina Inc., San Diego, CA, USA) following the manufacturers protocol.

Analysis of RNA-seq data

The transcriptome dataset, composed of sequencing reads, was generated by an Illumina NextSeq instrument. For every sample, quality control was carried out and assessed with the NGS Core Tools FastQC (<http://www.bioinformatics.babraham.ac.uk/projects/fastqc/>). Sequence reads were mapped using STAR (Dobin et al., 2013) and unmapped reads were remapped with Bowtie2 (Langmead and Salzberg, 2012) using the very sensitive local option. The total mapped reads were finally available in a BAM (Binary Alignment Map) format for raw read counts extraction. Read counts were generated by the htseq-count tool of the Python package HTSeq (Anders et al., 2015) with default parameters to generate an abundance matrix. At last, differential analyses were performed by the DESEQ2 (Love et al., 2014) package of the Bioconductor framework. Up- and down-regulated genes were selected based on the adjusted p value and the fold-change information. Gene expression was analyzed using dedicated R scripts to build volcano plots and. Heatmaps were built using the online application heatmapper (<http://www.heatmapper.ca/>). IPA (Ingenuity pathway analysis, Qiagen) was used for pathway analysis. Predictions of immune cell population from RNAseq data were made with the ImmQuant deconvolution software (Frishberg et al., 2016).

QUANTIFICATION AND STATISTICAL ANALYSIS

Following normality tests (Kolmogorov-Smirnov and Shapiro-Wilk), data were analyzed with a Mann-Whitney U-test or an unpaired t test (two-tailed unpaired) to compare two independent groups and non-parametric (Spearman) test for correlation analysis. Statistics were calculated with GraphPad 9.3.1 software. A probability (p) value of <0.05 was considered significant. *p < 0.05; **p < 0.01; ***p < 0.001; ****p < 0.0001.